New QM framework

Sergei Viznyuk

Abstract

I propose a model wherein a system is represented by a finite sequence of natural numbers. These numbers are thought of as population numbers in statistical ensemble formed as a sample with replacement of entities (microstates) from some abstract set. I derive the concepts of energy and of temperature. I show an analogy between energy spectra computed from the model and energy spectra of some known constructs, such as particle in a box and quantum harmonic oscillator. The presented model replaces the concept of wave function with *knowledge vector*. I derive Schrödinger-type equation for knowledge vector and discuss principal differences with Schrödinger equation. The model retains major QM hallmarks such as wave-particle duality, violation of Bell's inequalities, quantum Zeno effect, uncertainty relations, while avoiding controversial concept of wave function collapse. Unlike standard QM and Newtonian mechanics, the presented model has the Second Law of Thermodynamics built-in; in particular, it is not invariant with respect to time reversal.

As for prophecies, they will pass away; as for tongues, they will cease; as for knowledge, it will pass away.
1 Corinthians 13:8

1. PREAMBLE

Physical properties, such as temperature, energy, entropy, pressure, and phenomena such as Bose-Einstein condensation are exhibited not just by "real" physical systems, but also by virtual entities such as binary or character strings [1, 2, 3], world wide web [4], business and citation networks [5, 6], economy [7, 8, 9]. A characteristic quantum mechanical behavior has been observed in entities as different as electrons, electromagnetic waves, and nanomechanical oscillators [10].

There must be an underlying mechanism which accounts for the *grand commonality* in observed behavior of vastly different entities. *Scientists have recently discovered that various complex systems have an underlying architecture governed by shared organizing principles* [6]. The …*present-day quantum mechanics is a limiting case of some more unified scheme… Such a theory would have to provide, as an appropriate limit, something equivalent to a unitarily evolving state vector* $|\psi\rangle$ [11].

There are two factors present in all theories. One is the all-pervading *time*, and the other is the observer's *mind*. A successful *grand commonality* model must explain the nature of time, specify mechanism of how the *physical reality* projects onto the mind of observer, and relate time to that projection. A grand commonality theory may not contain fundamental physical constants. Any model containing such constants is deemed incomplete.

I call physical reality (i.e. the "real" world) the *underlying system*. The underlying system is represented by its state vector $\boldsymbol{x}$. The measuring device defines the *basis*. *Knowledge* vector $\boldsymbol{y}$ is the state vector $\boldsymbol{x}$ represented in the *basis*. The concept of knowledge vector may seem similar to wave function in Niels Bohr interpretation whence the wave function *is not to be taken seriously as describing a quantum-level physical reality, but is to be regarded as merely referring to our (maximal) "knowledge" of a physical system…* [11]. In the presented framework, the action of the

measuring device does not affect the state of underlying system, only the knowledge vector. The model does not exhibit the so-called measurement problem [12].

The state vector has an associated value of *proper time* [13] which serves as the ordering parameter for different states of underlying system. State vector is completely defined by a finite sequence of natural numbers (n_i). I call $\{n_i\}$ the *population numbers* of microstates $\{\boldsymbol{i}\}$ from set $\boldsymbol{G}$. I do not speculate what is microstate, or set $\boldsymbol{G}$, leaving them as abstract notions. I think of sequence (n_i) as a *sample with replacement* of microstates $\{\boldsymbol{i}\} \in \boldsymbol{G}$. I call such sample the *statistical ensemble*. Henceforth the notion of *physical reality* is reduced to a sequence of natural numbers (n_i) which do not have to be physicalized in any way.

The *proper time* has been previously defined [13] as the ordering parameter for the states of statistical ensemble:

$$t = \ln N \qquad \text{, where} \qquad N = \sum_{i \in \boldsymbol{G}} n_i \tag{1}$$

The proper time is quantized with time quantum $\tau = \Delta(\ln N) = 1/N$. I combine this definition of time with the following rule on time increments:

The positive $\Delta t > 0$ direction of time change is when:

$$\Delta N = \Delta N|_{\Delta t > 0} \equiv \sum_{\Delta n_i > 0} \Delta n_i \tag{2}$$

, where all Δn_i are non-negative.

The negative $\Delta t < 0$ direction of time change is when:

$$\Delta N = \Delta N|_{\Delta t < 0} \equiv \sum_{\Delta n_i < 0} \Delta n_i \tag{3}$$

, where all Δn_i are non-positive.

If (n_i) and (n_i') are such that some $\Delta n_i = n_i' - n_i$ are positive and some are negative, then state vectors (n_i) and (n_i') do not connect by timeline. There can be multiple timelines (histories) connecting two state vectors, as well as none.

For the given state vector, a choice of observation basis defines the *knowledge vector*. An observation basis associated with the measuring apparatus is the *preferred basis*, much discussed recently [14].

Commonly, the [Schrödinger] equation is solved in time-forward manner: given *known* state, find conditional probabilities of [future] measurement outcomes. Similarly, if same equation is solved backward in time, one would find the *past* too is only defined in terms of conditional probabilities, expressed as a modulus square of correlation function of two state vectors.

Any *known fact* from the past is deemed an artifact of the present state. What observer thinks as the *past*, the *present*, or the *future* is represented by the knowledge vectors in the *present*. This stance aligns with empirical evidence, e.g. from delayed-choice experiments [15], suggesting the history is determined by the setup at present. Thus, there is only *present*. A statistical correlation between knowledge vectors, having Δt as correlation distance, is perceived as *time evolution*.

To further develop the model, I derive the notions of energy in Section 2, and of temperature in Section 3. In Section 4 I derive the equation of motion for knowledge vector and discuss its similarity and differences with Schrödinger equation. I define the concept of measurement. I touch upon the notions of open/closed systems; conservation of energy; Bell's inequalities; Haag's theorem; quantum Zeno effect; and the notion of memory. I show the condition for quantum vs. classical behavior is the existence of predictable phase relationship between knowledge vectors.

2. ENERGY

The base tenet of the model is that the sequence $(n_{i \in \boldsymbol{G}})$ completely defines the underlying system. I call (n_i) sequence the *mode*. Since *mode* is formed as a sample with replacement, the [unconditional] probability of finding underlying system in a particular mode is given by the

multinomial probability mass function:

$$P\big((n_i);\ N,(p_i)\big) = N!\prod_{\boldsymbol{i}\in\boldsymbol{G}}\frac{p_i^{n_i}}{n_i!} \tag{4}$$

, where p_i is the probability of sampling microstate $\boldsymbol{i}$ from set $\boldsymbol{G}$. Within the context of the model

$$p_i = \frac{1}{M} \quad \forall\ \boldsymbol{i}\in\boldsymbol{G} \tag{5}$$

, where M is the cardinality of set $\boldsymbol{G}$. I introduce functions $\mathcal{E},\ \mu$ as follows:

$$\ln P\big((n_i);\ N,(p_i)\big) = \mu\big(N,(p_i)\big) - \mathcal{E}\big((n_i);\ N,(p_i)\big) \tag{6}$$

$$\mu\big(N,(p_i)\big) = \ln P\big((n_i \equiv N\cdot p_i);\ N,(p_i)\big) = N\cdot\big[H_\Omega\big(N,(p_i)\big) - H_S(p_i)\big] \tag{7}$$

$$H_\Omega\big(N,(p_i)\big) = \frac{1}{N}\left[\ln\Gamma(N+1) - \sum_{i\in\boldsymbol{G}}\ln\Gamma(Np_i+1)\right] \tag{8}$$

$$\mathcal{E}\big((n_i);\ N,(p_i)\big) = \mu\big(N,(p_i)\big) - \ln P\big((n_i);\ N,(p_i)\big) = \sum_{i\in\boldsymbol{G}}\left[\ln\frac{\Gamma(n_i+1)}{\Gamma(Np_i+1)} + (Np_i - n_i)\cdot\ln p_i\right] \tag{9}$$

$$\mathcal{E}\big((n_i);\ N,(p_i)\big) \geq 0; \qquad \mathcal{E}\big((n_i = Np_i\ \forall\ \boldsymbol{i}\in\boldsymbol{G});\ N,(p_i)\big) = 0 \tag{10}$$

, where $\Gamma(x)$ is *gamma* function, $H_S\big((p_i)\big) = -\sum_{i\in\boldsymbol{G}} p_i\ln p_i$ is Shannon's [16] entropy, and $H_\Omega\big(N,(p_i)\big)$ is equilibrium *microstate* entropy [17]. With (7-9), I rewrite (4) as

$$P\big((n_i);\ N,(p_i)\big) = exp\left(\mu\big(N,(p_i)\big) - \mathcal{E}\big((n_i);N,(p_i)\big)\right) \tag{11}$$

From (11) the probability of observing statistical ensemble of N microstates in a particular *mode* is determined solely by the value of $\mathcal{E}\big((n_i);N,(p_i)\big)$. If I'm to use $\mathcal{E}$ as a single independent variable, I can write the probability mass function in $\mathcal{E}$ domain as:

$$P\big(\mathcal{E};N,(p_i)\big) = g\big(\mathcal{E};N,(p_i)\big)\cdot exp\big(\mu\big(N,(p_i)\big) - \mathcal{E}\big) \tag{12}$$

Here $g\big(\mathcal{E};N,(p_i)\big)$ is the multiplicity (degeneracy) of the given $\mathcal{E}$ value[1], i.e. a number of ways the same value of $\mathcal{E}$ is realized by different modes with given parameters $N,(p_i)$. There is no analytic expression for $g\big(\mathcal{E};N,(p_i)\big)$, however, it is numerically computable. Table 1 contains $\mathcal{E}$, $g\big(\mathcal{E};N,(p_i)\big)$ values calculated for several sets of parameters $N,(p_i)$. Figures 1-2 show distinct values of $\mathcal{E}$ in increasing order for several values of parameter N and probabilities (5) calculated from (9), using algorithm [18] for finding partitions (n_i) of integer N into $\leq M$ parts [19]. The sum of $g\big(\mathcal{E};N,(p_i)\big)$ over all distinct values of $\mathcal{E}$ is the total number of modes. It is equal to the number of ways to distribute N indistinguishable balls into M distinguishable cells:

$$L(N,M) = \sum_{\{\mathcal{E}\}} g\big(\mathcal{E};N,(p_i)\big) = \frac{(N+M-1)!}{N!\,(M-1)!} \tag{13}$$

, where sum is over all distinct values of $\mathcal{E}$. Figure 3 shows the total number $L(N,M)$ of distinguishable states of statistical ensemble, and the total number of distinct values $\{\mathcal{E}\}$ as

[1] For a case of statistical ensemble with microstate probabilities (5); the multiplicity of $\mathcal{E}$ is the multiplicity of the value of multinomial coefficient in (4) [80]

functions of N for two sets of probabilities (5), calculated from (13) and (9) using algorithm [18]. The graphs demonstrate the following:

- For probabilities (5), the average degeneracy of $\{\mathcal{E}\}$ levels approaches $M!$ as $N \to \infty$.

This statement can be expressed as:

$$M! \cdot \lim_{N\to\infty} \sum_{\{\mathcal{E}\}} 1 = \frac{(N+M-1)!}{N!\,(M-1)!} \tag{14}$$

Here $\sum_{\{\mathcal{E}\}} 1$ sum represents the number of distinct values of $\mathcal{E}$ for the given parameters N, M. As $g(\mathcal{E}; N, (p_i))$ is not a smooth function of $\mathcal{E}$ (see Table 1), there could be no true probability density in $\mathcal{E}$ domain. However, I shall derive pseudo probability density to be used in expressions involving integration by $\mathcal{E}$ in *thermodynamic limit*. To be able to use analytical math, I have to extend (7-11) from discrete variables (n_i) to continuous domain. I call

- *Thermodynamic limit* is the approximation of large population numbers:

$$n_i \gg 1 \;\; \forall \;\; \boldsymbol{i} \in \boldsymbol{G} \tag{15}$$

In thermodynamic limit, I shall use Stirling's approximation for factorials

$$\ln n! \approx \frac{1}{2}\ln 2\pi n + n\ln n - n \tag{16}$$

With (5) it allows rewriting of (7-9) as

$$\mu(N,(p_i)) \cong -\frac{1}{2}\left[(M-1)\cdot \ln 2\pi N + \ln \prod_{\boldsymbol{i}\in\boldsymbol{G}} p_i\right] = \mu(N,M) = \frac{M}{2}\ln M - \frac{M-1}{2}\ln 2\pi N \tag{17}$$

$$\mathcal{E}((n_i);\; N,(p_i)) \cong \sum_{\boldsymbol{i}\in\boldsymbol{G}} \left(n_i + \frac{1}{2}\right)\cdot \ln\frac{n_i}{Np_i} = \sum_{\boldsymbol{i}\in\boldsymbol{G}} \left(n_i + \frac{1}{2}\right)\cdot \ln n_i - \left(N + \frac{M}{2}\right)\ln\frac{N}{M} \tag{18}$$

Figure 4 demonstrates function $\mu(N,(p_i))$ calculated for two sets of parameters (p_i) using exact expression (7) and approximate formula (17). In thermodynamic limit, $\mathcal{E}$ is a smooth function of (n_i) approximated by positive semi-definite quadratic form of $\{n_i - Np_i\}$ in the vicinity of its minimum (10):

$$\mathcal{E} \cong \sum_{\substack{\boldsymbol{i}\in\boldsymbol{G}\\ \boldsymbol{j}\in\boldsymbol{G}}} b_{i,j}\cdot(n_i - Np_i)\cdot(n_j - Np_j) \tag{19}$$

Knowing the covariance matrix [20] of multinomial distribution (4) allows reduction of (19) to diagonal form. The covariance matrix, divided by N is:

$$\sigma_{ij} = \delta_{ij}\cdot p_j - p_i\cdot p_j \qquad \text{, where} \qquad \delta_{i=j} = 1 \quad ; \; \delta_{i\neq j} = 0 \tag{20}$$

The rank of σ_{ij} is $M-1$. If d_{ij} is a diagonal form of σ_{ij}, the eigenvalues of σ_{ij} are $d_i = d_{ii}$:

$$d_{ij} = diag(\sigma_{ij}) \quad ; \quad d_i = d_{ii} \quad ; \quad d_1 \equiv 0 \quad ; \quad d_{i>1} > 0 \tag{21}$$

For equal probabilities (5), $d_{i>1} = 1/M$. I transform to new discrete variables:

$$x_{i>1} = \sum_{\boldsymbol{j}\in\boldsymbol{G}} (n_j - Np_j)\frac{\Theta_{ji}}{\sqrt{d_i}} = \sqrt{M}\sum_{\boldsymbol{j}\in\boldsymbol{G}} \left(n_j - \frac{N}{M}\right)\cdot\Theta_{ji} \qquad ; x_1 \equiv 0 \tag{22}$$

, where Θ_{ij} is matrix with columns as unit eigenvectors of σ_{ij} corresponding to eigenvalues (21). In case of $M = 3$ and probabilities (5)

$$\Theta_{ij} = \begin{bmatrix} 1/\sqrt{3} & -1/\sqrt{6} & 1/\sqrt{2} \\ 1/\sqrt{3} & -1/\sqrt{6} & -1/\sqrt{2} \\ 1/\sqrt{3} & \sqrt{2/3} & 0 \end{bmatrix} \tag{23}$$

The eigenvector Θ_{i1} corresponding to eigenvalue $d_1 \equiv 0$ is perpendicular to hyper-plane (1) defined by $\sum_{i\in \boldsymbol{G}} n_i = N$ in M-dimensional space of (n_i) coordinates, while vector $(n_i - Np_i)$ is parallel to the hyper-plane. Therefore, $x_1 \equiv 0$ in (22). I rewrite (19) in terms of new variables $\{x_i\}$ as

$$\mathcal{E} = \frac{1}{2N}\sum_{\boldsymbol{i}\in \boldsymbol{G}} x_i^2 = \frac{\langle \boldsymbol{x}|\boldsymbol{x}\rangle}{2N} \tag{24}$$

I call $\{x_i\}$ the *canonical variables* of statistical ensemble, and $\boldsymbol{x} = (x_i)$ the *canonical state vector*. I call parameter $\mathcal{E}$ the *energy* of statistical ensemble. If statistical ensemble of N microstates is divided into K sub-ensembles of $\{N_k\}$ microstates as

$$N = \sum_{k=1}^{K} N_k = \sum_{k=1}^{K}\sum_{\boldsymbol{i}\in \boldsymbol{G}} (n_i)_k \tag{25}$$

, then, from (22,25), the relation between canonical vector $\boldsymbol{x}$ of the larger system and vectors $\{\boldsymbol{x}_k\}$ of subsystems is:

$$\boldsymbol{x} = \sum_{k=1}^{K} \boldsymbol{x}_k \tag{26}$$

I may also call $\boldsymbol{x}$ the *canonical momentum* of the system. Relation (26) states the total momentum $\boldsymbol{x}$ of the system equals the sum of momenta of constituent parts. The expressions (22,24) lead to the following time evolution laws for $\boldsymbol{x}$, $\mathcal{E}$, with time t defined as proper time (1):

$$\begin{gathered} |\boldsymbol{x}(N+1) - \boldsymbol{x}(N)|^2 = M - 1 \quad ; \quad \langle\frac{\partial \boldsymbol{x}}{\partial t}\rangle = 0 \quad ; \quad \langle\frac{\partial \boldsymbol{x}^2}{\partial t}\rangle = (M-1)\cdot N \\ \langle\frac{\partial \mathcal{E}}{\partial t}\rangle = \frac{M-1}{2} - \mathcal{E} \quad ; \quad \langle\mathcal{E}(t)\rangle = \frac{M-1}{2} + \left(\mathcal{E}(t_0) - \frac{M-1}{2}\right)\cdot exp(t_0 - t) \end{gathered} \tag{27}$$

, where $\langle q\rangle$ designates the *expectation value* of q. The canonical vector $\boldsymbol{x}$ constitutes the *knowledge vector* in the basis of eigenvectors of σ_{ij}. As the *basis* is associated with an observer, basis vectors may differ from eigenvectors of σ_{ij}. If the basis is obtained from eigenvectors of σ_{ij} via an orthogonal transformation, linear form (26), and quadratic form (24) are preserved. Hence, I state the *conservation of energy law* as follows: *the energy of the system is conserved under orthogonal transformations of the basis*. In layman's terms, it means the energy may change from one form to another (e.g. from potential into kinetic), while total energy of the system is conserved under such transformation. The conservation of energy law in this form differs from the common one (Conservation of Energy, Wikipedia) which "… *states that the total energy of an isolated system remains … conserved over time*". From (27) it follows the expectation value of energy $\langle\mathcal{E}(t)\rangle$ *is not conserved over time*. However, in scenarios drawn from classical physics, the exponent in (27) has much longer characteristic timescale than orthogonal transformation of observation basis. This condition is equivalent to $(\Delta t \cong \Delta N/N) \ll 1$, i.e. to *thermodynamic limit* case.

Figure 5 demonstrates function $\sqrt{\mathcal{E}/N}$ calculated for two sets of parameters (p_i) using exact expression (9) and approximations (18), and (24). I plotted $\sqrt{\mathcal{E}/N}$ instead of $\mathcal{E}$ to show asymptotic behavior of (9) and (18) in comparison with quadratic form (24). Using (17) and (24) I obtain multivariate normal approximation [20] to multinomial distribution (4) as

$$P\big((x_i);\, N, (p_i)\big) \cong (2\pi N)^{\frac{1-M}{2}} \cdot exp\left[-\sum_{\boldsymbol{i}\in \boldsymbol{G}}\left(\frac{x_i^2}{2N} + \frac{\ln p_i}{2}\right)\right] = exp\left[\mu\big(N,(p_i)\big) - \sum_{\boldsymbol{i}\in \boldsymbol{G}}\frac{x_i^2}{2N}\right] \tag{28}$$

Figure 6 shows graphs of $\ln P\big((n_i); N, (p_i)\big)$ as a function of n_1 calculated for $N = 1000$ and four sets of probabilities (p_i), using exact formula (4), and multivariate normal approximation (28).

In order to derive pseudo probability density in $\mathcal{E}$ domain, I note that:

- In thermodynamic limit, the number $L(\mathcal{E}_0; N, M)$ of distinguishable states of statistical ensemble having $\mathcal{E} \le \mathcal{E}_0$ is proportional to the volume of $(M-1)$ –dimensional sphere of radius $\sqrt{2N\mathcal{E}_0}$. This statement can be expressed as

$$L(\mathcal{E}_0; N, M) = \lim_{N\to\infty} \sum_{\{\mathcal{E}\}\le\mathcal{E}_0} g(\mathcal{E}; N, M) = a(N, M) \cdot (2N\mathcal{E}_0)^{\frac{M-1}{2}} \tag{29}$$

The sum in (29) is over all distinct values of $\mathcal{E}$ which are less or equal than $\mathcal{E}_0$. The function $a(N, M)$ is determined from normalization requirement:

$$1 = \sum_{\{\mathcal{E}\}} P(\mathcal{E}; N, M) = \sum_{\{\mathcal{E}\}} g(\mathcal{E}; N, M) \cdot exp(\mu(N, M) - \mathcal{E}) \tag{30}$$

In order to convert from sums to integrals over continuous variable $\mathcal{E}$, I define pseudo density $g(\mathcal{E}; N, M)$ of distinguishable states of statistical ensemble as

$$g(\mathcal{E}; N, M) = \frac{\partial}{\partial\mathcal{E}} L(\mathcal{E}; N, M) = a(N, M) \cdot \frac{M-1}{2} \cdot (2N)^{\frac{M-1}{2}} \cdot \mathcal{E}^{\frac{M-3}{2}} \tag{31}$$

The corresponding pseudo probability density $P(\mathcal{E}; N, M)$ is given by (12). The normalization requirement for these functions becomes:

$$1 = \int_0^{\mathcal{E}_{max}} P(\mathcal{E}; N, M) d\mathcal{E} = \int_0^{\mathcal{E}_{max}} g(\mathcal{E}; N, M) \cdot exp(\mu(N, M) - \mathcal{E}) d\mathcal{E} \tag{32}$$

The $\mathcal{E}_{max}$ value is obtained from (9) by having microstate $\boldsymbol{j}$ with lowest probability $p_{min} = \min_{\boldsymbol{i}\in\boldsymbol{G}}\{p_i\}$ acquire maximum population: $n_{max} = N;\ n_{i\neq j} = 0$. From (9), as $N \to \infty$:

$$\mathcal{E}_{max}\big((n_i);\ N, (p_i)\big) \cong -N \cdot \ln p_{min} \tag{33}$$

For probabilities (5):

$$\mathcal{E}_{max}\big((n_i);\ N, M\big) \cong N \cdot \ln M \tag{34}$$

From (33) $\mathcal{E}_{max} \to \infty$ as $N \to \infty$. That allows replacing $\mathcal{E}_{max}$ in the upper limit of integral in (32) with ∞. I get [20] the expression for function $a(N, M)$ in (29) as:

$$a(N, M) = \left[e^{\mu(N,M)} \cdot (2N)^{\frac{M-1}{2}} \cdot \int_0^\infty \mathcal{E}^{\frac{M-1}{2}} e^{-\mathcal{E}} d\mathcal{E}\right]^{-1} = \frac{e^{-\mu(N,M)}}{(2N)^{\frac{M-1}{2}} \Gamma\left(\frac{M+1}{2}\right)} \tag{35}$$

Using (35) and (17) allows rewriting (29) as

$$L(\mathcal{E}; N, M) = \frac{\mathcal{E}^{\frac{M-1}{2}}}{\Gamma\left(\frac{M+1}{2}\right)} e^{-\mu(N,M)} = \frac{(2\pi N\mathcal{E})^{\frac{M-1}{2}}}{M^{\frac{M}{2}} \cdot \Gamma\left(\frac{M+1}{2}\right)} = \frac{V\left(\sqrt{2N\mathcal{E}}; M-1\right)}{M^{\frac{M}{2}}} \tag{36}$$

, where $V\left(\sqrt{2N\mathcal{E}}; M-1\right) = \dfrac{(2\pi N\mathcal{E})^{\frac{M-1}{2}}}{\Gamma\left(\frac{M+1}{2}\right)}$ is the volume of $(M-1)$ –dimensional sphere of radius $\sqrt{2N\mathcal{E}}$.

The number $n(\mathcal{E})$ of distinct values of $\mathcal{E}$ in $N \to \infty$ limit can be estimated from (36) and (14) as

$$n(\mathcal{E}) = \frac{L(\mathcal{E}; N, M)}{M!} = \frac{(2\pi N\mathcal{E})^{\frac{M-1}{2}}}{M^{\frac{M}{2}} \cdot \Gamma\left(\frac{M+1}{2}\right) \Gamma(M+1)} \tag{37}$$

From (37) one can approximately enumerate distinct energy levels $\mathcal{E}_n$ by "quantum number" n:

$$\mathcal{E}_n = \left[\Gamma\left(\frac{M+1}{2}\right)\Gamma(M+1)e^{\mu(N,M)} \cdot n\right]^{\frac{2}{M-1}} = \frac{M}{2\pi N}\left[\Gamma\left(\frac{M+1}{2}\right)\Gamma(M+1)M^{\frac{1}{2}} \cdot n\right]^{\frac{2}{M-1}} \tag{38}$$

From (31) the pseudo density $g(\mathcal{E}; N, M)$ of distinguishable states of statistical ensemble is

$$g(\mathcal{E}; N, M) = \frac{\partial}{\partial \mathcal{E}} L(\mathcal{E}; N, M) = \frac{\mathcal{E}^{\frac{M-3}{2}} e^{-\mu(N,M)}}{\Gamma\left(\frac{M-1}{2}\right)} \tag{39}$$

I use condition (13) to define effective $\mathcal{E}_{max}^{eff}$ value:

$$L(N, M) = L\left(\mathcal{E}_{max}^{eff}; N, M\right) = \frac{\mathcal{E}_{max}^{eff\ \frac{M-1}{2}}}{\Gamma\left(\frac{M+1}{2}\right)} e^{-\mu(N,M)} = \frac{(N+M-1)!}{N!\,(M-1)!} \tag{40}$$

Figure 7 shows $L(\mathcal{E}; N, \{p_i\})$ calculated from exact expressions (4), (9), and from formula (36). From (11), (17), and (39), the pseudo probability density function of statistical ensemble in thermodynamic limit is

$$P(\mathcal{E}; N, M) = \frac{\mathcal{E}^{\frac{M-3}{2}} e^{-\mathcal{E}}}{\Gamma\left(\frac{M-1}{2}\right)} = \gamma_{b,c}(\mathcal{E}); \qquad b = 1;\ \ c = \frac{M-1}{2} \tag{41}$$

, where $\gamma_{b,c}(\mathcal{E})$ is the probability density function of *gamma* [20] distribution with scale parameter $b = 1$, and shape parameter $c = (M-1)/2$. I calculate moments of $\mathcal{E}$:

Mean:
$$\langle \mathcal{E} \rangle = \sum_{\{n_i\}} \mathcal{E}\big((n_i);\ N, M\big) \cdot P\big((n_i);\ N, M\big) \tag{42}$$

Variance:
$$\sigma_{\mathcal{E}}^2 = \sum_{\{n_i\}} \big(\mathcal{E}\big((n_i); N, M\big) - \langle \mathcal{E} \rangle\big)^2 \cdot P\big((n_i); N, M\big) \tag{43}$$

r^{th} moment about mean:
$$\kappa_r(N, M) = \sum_{\{n_i\}} \big(\mathcal{E}\big((n_i);\ N, M\big) - \langle \mathcal{E} \rangle\big)^r \cdot P\big((n_i);\ N, M\big) \tag{44}$$

The sums in (42-44) are over all combinations of (n_i) satisfying (1), i.e. over all partitions of N. Expression (41) allows explicit calculation of all moments of $\mathcal{E}$ in thermodynamic limit. From (41) the mean value $\langle \mathcal{E} \rangle$, the variance $\sigma_{\mathcal{E}}^2$, and the third moment κ_3 are:

$$\langle \mathcal{E} \rangle = \frac{M-1}{2} \tag{45}$$

$$\sigma_{\mathcal{E}}^2 = \frac{M-1}{2} \tag{46}$$

$$\kappa_3 = M - 1 \tag{47}$$

Figure 8 shows calculations of mean value $\langle \mathcal{E} \rangle$, the variance $\sigma_{\mathcal{E}}^2$, and the third moment κ_3 from the exact expressions (42-44) for the moments, with (4) as probability mass function. It demonstrates how these values asymptotically approach thermodynamic limit values (45-47) as $N \cdot p_i \to \infty$, i.e. as $t \to \infty$ where t is the proper time (1).

I shall demonstrate how the presented model correlates with some known constructs. Consider one-dimensional quantum harmonic oscillator. Its energy levels [21] are given by:

$$\mathcal{E}_n = \left(n + \frac{1}{2}\right) \cdot \hbar\omega \tag{48}$$

, where ω is the base frequency, and $n = 0,1,2 \ldots$. Energy levels (48) are equally-spaced. In my model, similar pattern is exhibited by energy levels of statistical ensemble of cardinality $M = 3$, as shown on Figure 1. From (18) in thermodynamic limit approximation, the energy of statistical ensemble can be written as:

$$\mathcal{E} = \sum_{i \in \boldsymbol{G}} \frac{{\Delta_i}^2}{2 \cdot \langle n \rangle} \tag{49}$$

, where

$$\Delta_i = n_i - \langle n \rangle \quad ; \quad \sum_i \Delta_i = 0 \quad ; \quad \langle n \rangle = \frac{N}{M} \tag{50}$$

From above, the energy levels of statistical ensemble of cardinality $M = 3$ are:

$$\mathcal{E}_k = \frac{L_k}{N} \tag{51}$$

, where L_k are *Loeschian numbers* [22]. With (48) and (51), I can write the comparison table of the first few energy levels of quantum harmonic oscillator in units of $\hbar\omega/2$, and of statistical ensemble of cardinality $M = 3$ in units $1/N$:

quantum harmonic oscillator		1	3		5	7	9	11		13	15		17	19	21	23	25	27		29	31	33	35		37	39	41	43
statistical ensemble of cardinality $M = 3$	0	1	3	4		7	9		12	13		16		19	21		25	27	28		31			36	37	39		43

, where black boxes designate missing energy levels. In the second row, the energy levels shown in shaded boxes are only realized for modes with $mod(N, 3) > 0$; and energy levels shown in white boxes are realized for modes with $mod(N, 3) = 0$. Here $mod(N, 3)$ is the remainder of division of N by 3.

Consider another classic quantum mechanical example: particle of mass m in a box of size L. Its energy levels [21] are given by:

$$\mathcal{E}_n = \frac{h^2}{8mL^2} n^2 \quad ; \quad n = 1,2,3 \ldots \tag{52}$$

In my model, similar energy spectrum is exhibited by statistical ensemble of cardinality $M = 2$, as shown on Figure 2. From (49), the energy levels of statistical ensemble of cardinality $M = 2$, in thermodynamic limit approximation, are:

$$\mathcal{E}_n = \frac{n^2}{2N} = \frac{h^2}{8mL^2} n^2 \quad ; \quad n = 0,1,2 \ldots \tag{53}$$

, where $m = N \cdot \left(\frac{h}{2L}\right)^2$ is to be considered as the *effective mass* of the particle. (54)

Energy levels (53) with even n are only possible when N is even, and energy levels with odd n are only possible when N is odd. With ½ probability the lowest energy level is $\mathcal{E} = \mathcal{E}_0 = 0$, and with ½ probability it is $\mathcal{E} = \mathcal{E}_1 = 1$, in units of $h^2/(8mL^2)$.

3. THERMODYNAMIC ENSEMBLE

The statistical ensemble considered in previous section represents a single copy of underlying system, with mode $\boldsymbol{k} = (n_{i \in \boldsymbol{G}})$ uniquely identifying the state. In this section, I consider observation as a random pick of underlying system from a collection of systems, each represented by its own statistical ensemble of cardinality M. I call such collection of systems *thermodynamic ensemble*. I designate $\{\boldsymbol{k}\}$ the set of *modes* a system may occupy; K the total number of systems,

and K_k the number of systems in mode $\boldsymbol{k}$:

$$\sum_{\{k\}} K_k = K \tag{55}$$

I designate $exp\big(\rho(N)\big)$ the probability for a system to be in any mode with total population of microstates N. Then, from (11), the probability for a system to be in a mode $\boldsymbol{k}$ is:

$$p_k = exp\big(\rho(N) + \mu(N) - \mathcal{E}(\boldsymbol{k})\big) = exp(\rho_N + \mu_N - \mathcal{E}_{\boldsymbol{k}}) \tag{56}$$

I consider systems in the same mode $\boldsymbol{k}$ indistinguishable to the observer. Then the probability mass function of distribution of modes among systems is

$$P\big((K_k);\ K, (p_k)\big) = K! \prod_{\{k\}} \frac{p_k^{K_k}}{K_k!} \tag{57}$$

The objective is to find the most probable distribution (K_k). For standalone systems, the most probable distribution is the one which maximizes (57), i.e.

$$K_k = K \cdot p_k \tag{58}$$

Let's consider systems to be part of some bigger system in a certain state. That imposes conditions on distribution of modes among systems, so relations (45-47), (58) may no longer hold. I consider one of the possible conditions and show how it leads to the notion of *temperature*. Let the state of the bigger system be such that the average energy of the systems in thermodynamic ensemble is $\langle\mathcal{E}\rangle$, which may be different from the average energy of a standalone systems given by (45). Then:

$$\langle\mathcal{E}\rangle \cdot K = \sum_{\{k\}} K_k \cdot \mathcal{E}_{\boldsymbol{k}} \tag{59}$$

To find the most probable distribution of modes (K_k), I shall maximize logarithm of (57) using method of Lagrange multipliers [23, 24] with conditions (55) and (59):

$$\begin{aligned} \ln P\big((K_k);\ K, (p_k)\big) &= \ln\Gamma(K+1) + \sum_{\{k\}} [K_k \cdot \ln p_k - \ln\Gamma(K_k+1)] \\ &= \ln\Gamma(K+1) + \sum_{\{k\}} [K_k \cdot (\rho_N + \mu_N - \mathcal{E}_{\boldsymbol{k}}) - \ln\Gamma(K_k+1)] \end{aligned} \tag{60}$$

From (60), (59), (55) I obtain the following equation involving Lagrange multipliers α and β:

$$\Psi_0(K_k+1) = \rho_N + \mu_N - (1+\alpha) \cdot \mathcal{E}_{\boldsymbol{k}} - \beta \tag{61}$$

, where Ψ_0 is *digamma* function, and α and β are to be determined by solving (61) for K_k:

$$K_k = \Psi_0^{-1}\left(\rho_N + \mu_N - \frac{\mathcal{E}_{\boldsymbol{k}}}{T} - \beta\right) - 1 \tag{62}$$

, and by plugging K_k from (62) into (59) and (55). In (62), Ψ_0^{-1} is the inverse digamma function, and $1/T = 1 + \alpha$. The parameter T is commonly known as *temperature*.

Since the number of systems K_k in mode $\boldsymbol{k}$ cannot be negative, expression (62) effectively limits modes which can be present in most probable distribution to those satisfying

$$\rho_N + \mu_N - \frac{\mathcal{E}_{\boldsymbol{k}}}{T} - \beta + \gamma \geq 0 \tag{63}$$

, where $\gamma \cong 0.577215665$ is *Euler–Mascheroni* constant. Using approximation [25]: $exp\big(\Psi_0(K_k+1)\big) \cong K_k + 1/2$, I rewrite (62) as:

$$K_k \cong exp\left(\rho_N + \mu_N - \frac{\mathcal{E}_{\boldsymbol{k}}}{T} - \beta\right) - \frac{1}{2} \tag{64}$$

Presence of $-½$ term in (64) leads to a computationally horrendous task of calculating β and T, because the summation in (55) and (59) has to be only performed for modes satisfying (63). I shall leave the exact computation to a separate exercise, and make a shortcut, by ignoring $-½$ term in (64). This approximation is equivalent to Boltzmann's postulate[2] [26] that the number of systems in mode $\boldsymbol{k}$ is proportional to $exp(-\mathcal{E}_k/T)$. The shortcut allows calculation of Lagrange multiplier β from (55):

$$exp(-\beta) = \frac{K}{Z(T)} \quad \text{, where} \quad Z(T) = \sum_{\{k\}} exp\left(\rho_N + \mu_N - \frac{\mathcal{E}_k}{T}\right) \tag{65}$$

Using expression (39), the partition function $Z(T)$ in (65) can be evaluated as:

$$\begin{aligned} Z(T) &= \sum_{N=1}^{\infty} exp(\rho_N) \sum_{\{k\}_N} exp\left(\mu_N - \frac{\mathcal{E}_k}{T}\right) = \sum_{N=1}^{\infty} exp(\rho_N) \int_0^{\infty} g(\mathcal{E}; N, M)\, exp\left(\mu_N - \frac{\mathcal{E}}{T}\right) d\mathcal{E} \\ &= \sum_{N=1}^{\infty} exp(\rho_N) \int_0^{\infty} \frac{\mathcal{E}^{\frac{M-3}{2}}}{\Gamma\left(\frac{M-1}{2}\right)} exp\left(-\frac{\mathcal{E}}{T}\right) d\mathcal{E} = T^{\frac{M-1}{2}} \sum_{N=1}^{\infty} exp(\rho_N) = T^{\frac{M-1}{2}} \end{aligned} \tag{66}$$

The equation (59) then becomes

$$\langle \mathcal{E} \rangle = T^2 \cdot \frac{\partial}{T} \ln Z = \frac{M-1}{2} \cdot T \tag{67}$$

Eq. (67) is the familiar relation [24] between average per-particle energy and temperature in $(M-1)$-dimensional ideal Maxwell-Boltzmann gas. Thermodynamic entropy $S_{\boldsymbol{T}}$ can be evaluated as:

$$\begin{aligned} S_{\boldsymbol{T}} &= -\sum_{\{k\}} P_k(T) \cdot \ln P_k(T) = \frac{M-1}{2} \ln(eT) - \sum_{\{\mathrm{k}\}} (\rho_N + \mu_N) \cdot P_k(T) \\ &= \frac{M-1}{2} \ln(eT) - \sum_{N=1}^{\infty} (\rho_N + \mu_N) exp(\rho_N) \sum_{\{\mathrm{k}\}_N} \frac{exp\left(\mu_N - \frac{\mathcal{E}_k}{T}\right)}{Z(T)} \\ &= \frac{M-1}{2} \ln(eT) - \sum_{N=1}^{\infty} (\rho_N + \mu_N) \cdot exp(\rho_N) \end{aligned} \tag{68}$$

, where

$$P_k(T) = \frac{K_k}{K} = \frac{exp\left(\rho_N + \mu_N - \frac{\mathcal{E}_k}{T}\right)}{Z(T)} \tag{69}$$

With expression (17) for μ_N, in thermodynamic limit, I rewrite (68) as

$$S_{\boldsymbol{T}} = \frac{M-1}{2} \ln(2\pi eT) - \frac{M}{2} \ln M + S_{\boldsymbol{N}} + \frac{M-1}{2} \sum_N exp(\rho_N) \ln N \tag{70}$$

, where

$$S_N = -\sum_N \rho_N \cdot exp(\rho_N) \tag{71}$$

---

[2] While widely used, this postulate has rather unphysical consequence that there is a non-zero probability of finding a system in a mode with arbitrary large energy. Another consequence is the divergence of partition function for some constructs, e.g. hydrogen electronic levels [60].

To calculate S_N I have to make an assumption on $exp(\rho_N)$ distribution. As a possible example, I shall assume the number $N = \sum_{i \in \boldsymbol{G}} n_i$ of microstates for a system in thermodynamic ensemble is Poisson-distributed around mean $\langle N \rangle \gg 1$ value. Therefore, for S_N, I can use expression for the entropy of Poisson distribution [27]:

$$S_N \cong \frac{1}{2} \ln(2\pi e \cdot \langle N \rangle) \tag{72}$$

I also use the following:

$$\sum_N exp(\rho_N) \ln N = \langle \ln N \rangle \cong \ln \langle N \rangle \tag{73}$$

With (72), (73) I finally obtain:

$$S_{\boldsymbol{T}} = \frac{M}{2} \ln\left(2\pi e \frac{\langle N \rangle}{M}\right) + \frac{M-1}{2} \ln T \tag{74}$$

In case of $M = 4$, i.e. for $(M-1) = 3$ degrees of freedom, the expression (74) turns into equivalent of Sackur-Tetrode equation [28] for entropy of ideal gas. For thermodynamic entropy of a standalone system, instead of (68-74) from (17) and (45) I have:

$$\begin{aligned} S = -\sum_{\{k\}} P_k \cdot \ln P_k = -\sum_{\{k\}} exp(\mu_N - \mathcal{E}_k) \cdot (\mu_N - \mathcal{E}_k) = \langle \mathcal{E} \rangle - \mu_N \\ = \frac{M-1}{2} - \frac{M}{2} \ln M + \frac{M-1}{2} \ln 2\pi N = \frac{M}{2} \ln\left(2\pi e \frac{N}{M}\right) - \frac{1}{2} \ln 2\pi e N \end{aligned} \tag{75}$$

Thermodynamic entropy (74) per system in thermodynamic ensemble is larger than entropy (75) of a standalone system by term (72) plus the temperature-related term. The increase in entropy by S_N happens because of the spread in values of N, i.e. in *age* of the systems. The increase in entropy by temperature-related term $\frac{M-1}{2} \ln T$ is due to the spread in energies of the systems. The non-zero thermodynamic entropy of a standalone system implies its state is unknown prior to observation, for each observation. Using (1) I rewrite (75) in terms of proper time t as:

$$S(t; M) = S_0(M) + \frac{M-1}{2} t \quad \text{, where} \quad S_0(M) = \frac{M-1}{2} \ln 2\pi e - \frac{M}{2} \ln M \tag{76}$$

The expression for $S_0(M)$ in (76) was derived in thermodynamic limit, i.e. when $N \to \infty$. When $N = 1$ (i.e. when $t = 0$) $S = \ln M$. By comparing $S_0(M)$ to $\ln M$ (Figure 9) I see that $S_0(M)$ fairly close to $\ln M$ except when M is large enough, in which case thermodynamic limit approximation for the given N becomes less valid anyhow. Therefore, I can replace $S_0(M)$ with $\ln M$ in (76) and obtain thermodynamic entropy of a standalone system as:

$$S(t; M) = \ln M + \frac{M-1}{2} t \tag{77}$$

The [linear] relation between thermodynamic entropy and proper time (77) is the manifestation of the Second Law of Thermodynamics (SLT). Previously, SLT has been demonstrated in the context of time model [13] using numeric calculation of *microstate entropy*.

The expression for $Z(T)$ in (66) has been derived in thermodynamic limit approximation, i.e. when $N \to \infty$. It means there must be large number of energy levels included in sum (65), i.e. temperature T cannot be too small. Therefore, the expressions (66-67) are only valid for $T \gg \Delta\mathcal{E}$, where $\Delta\mathcal{E}$ is the characteristic difference between adjacent energy levels.

For statistical ensemble of cardinality $M = 3$ the approximately evenly-spaced energy levels (Figure 1) allow for more accurate expression for partition function. From (38) the characteristic difference between energy levels in the limit $N \to \infty$ is:

$$\Delta\mathcal{E} = \frac{M!}{g(\mathcal{E}; N, M)} = 6 \cdot exp(\mu_N) = \frac{18\sqrt{3}}{2\pi N} \cong \frac{5}{N} \tag{78}$$

Figure 10 shows numeric calculation of the difference $\Delta\mathcal{E}$ between adjacent energy levels averaged over distinct states of statistical ensemble with the given value of N, and $M = 3$.

If $mod(N, 3) = 0$, the first 17 energy levels in units of $(\hbar\omega/2 = 1/N)$ and their degeneracy:

k	0	1	2	3	4	5	6	7	8	9	10	11	12	13	14	15	16
$\mathcal{E}_k$	0	3	9	12	21	21	27	36	39	39	48	57	57	63	63	75	81
g_k	1	6	6	6	6	6	6	6	6	6	6	6	6	6	6	6	6

If $mod(N, 3) > 0$, the first 16 energy levels and their degeneracy:

k	1	2	3	4	5	6	7	8	9	10	11	12	13	14	15	16
$\mathcal{E}_k$	1	4	7	13	16	19	25	28	31	37	43	49	52	61	64	67
g_k	3	3	6	6	3	6	3	6	6	6	6	9	6	6	3	6

The combined energy levels are thus given by (51). I can use (48) as approximation for the combined energy levels (51) in expression for partition function (65) with degeneracy of each level $g = M!$=6, and obtain the mean energy of modes for subsystems with given N as [29]:

$$\langle\mathcal{E}\rangle_\omega = \frac{\hbar\omega}{2} + \frac{\hbar\omega}{\exp\left(\frac{\hbar\omega}{T}\right) - 1} \qquad ; \ \hbar\omega = 2/N \tag{79}$$

The relation $\langle\mathcal{E}\rangle_\omega/\hbar\omega$ is commonly referred to as the average number of photons in a mode [30]. In my model, the notion of a photon is meaningless. The quantized energy levels (9,48,51) make transitions between modes appear as absorption or emission of particles.

Formula (79) has been obtained using linear dependence (48) of energy levels $\mathcal{E}_n$ on *quantum number* n, in $N \gg 1$, i.e. $\hbar\omega \ll 1$ limit. Figure 1 shows approximation (48) holds reasonably well when n is not too large. From (14), the linearity (48) break down for $n \geq N^2/24$. Therefore, the typical black-body spectrum can only be exhibited by relatively low-temperature systems, with $(\hbar\omega{\sim}T) \ll 1$. A good example is the cosmic microwave background. The higher the temperature, the more will the spectrum differ from that of black body, especially in $\hbar\omega > T$ region, where spectral intensity would fall off steeper than black-body radiation as $\hbar\omega \to \infty$. Such deviation from black-body radiation is already obvious in solar spectrum.

Zero-point energy term $\hbar\omega/2$ in (79) is the subject of a hundred-year controversy [31, 32]. It leads to the infinite energy density of the field in any volume of space, as there is no upper limit on ω in conventional theory. In presented model, contrary to the conventional theory, $\hbar\omega$ term cannot contribute more than $(1/N) \leq 1$ to the average energy (79), i.e. its contribution is within standard deviation (46). The problem of infinite zero-point energy [31] does not exist within the context of the model.

4. THE DYNAMICS OF KNOWLEDGE VECTOR

In this section, I discuss dynamics of knowledge vector in the context of time model (1). A knowledge vector is defined in an observation basis associated with the measuring device. A special interest presents knowledge vector $\boldsymbol{z}$ as $SO(M-1)$ projection $\boldsymbol{\Theta}$ of canonical vector $\boldsymbol{x}$ (22)

$$\boldsymbol{z} = \boldsymbol{\Theta}^{\boldsymbol{T}} \cdot \boldsymbol{x} \tag{80}$$

Transformation (80) preserves quadratic form (24) which means the components $\{z_i\}$ have familiar from classical mechanics relation to energy. The orthogonal transformation $\boldsymbol{\Theta}$ in (80) represents the measuring device. The state of measuring device has to reflect the state of underlying system. Therefore, transformation $\boldsymbol{\Theta}(t, \boldsymbol{x})$ depends on $\boldsymbol{x}$, and, possibly, proper time t. Any $SO(M-1)$ matrix $\boldsymbol{\Theta}$ can be expressed [33] as matrix exp() of real skew-symmetric matrix $\boldsymbol{A}$:

$$\boldsymbol{\Theta} = exp(\boldsymbol{A}) \qquad \text{, where } A_{ij} = -A_{ji} \tag{81}$$

Any real skew-symmetric matrix $\boldsymbol{A}$ can be reduced [33, 34] to a block-diagonal form $\boldsymbol{D}$ by $SO(M-1)$ transformation:

$$\boldsymbol{A} = \boldsymbol{O} \cdot \boldsymbol{D} \cdot \boldsymbol{O^T} \tag{82}$$

, where

$$\boldsymbol{D} = \begin{pmatrix} 0 & 0 & 0 & & & \\ 0 & 0 & \varphi_1 & \cdots & 0 & \\ 0 & -\varphi_1 & 0 & & & \\ & \vdots & & \ddots & \vdots & \\ & & & 0 & \varphi_n & \\ & 0 & & \cdots & -\varphi_n & 0 \end{pmatrix} \text{, and } \varphi_k = \varphi_k(t, \boldsymbol{x}) \text{ are real} \tag{83}$$

Plugging (82) into (81) I obtain from (80):

$$\boldsymbol{z} = \boldsymbol{O} \cdot exp(\boldsymbol{D^T}) \cdot \boldsymbol{O^T} \cdot \boldsymbol{x} \tag{84}$$

, where

$$exp(\boldsymbol{D^T}) = \begin{pmatrix} 1 & 0 & 0 & & & \\ 0 & cos(\varphi_1) & -sin(\varphi_1) & \cdots & 0 & \\ 0 & sin(\varphi_1) & cos(\varphi_1) & & & \\ & \vdots & & \ddots & \vdots & \\ & & & cos(\varphi_n) & -sin(\varphi_n) & \\ & 0 & & \cdots & sin(\varphi_n) & cos(\varphi_n) \end{pmatrix} \tag{85}$$

I re-write (84) as

$$\boldsymbol{y} = \boldsymbol{O^T} \cdot \boldsymbol{z} = exp(\boldsymbol{D^T}) \cdot \boldsymbol{O^T} \cdot \boldsymbol{x} = exp(\boldsymbol{D^T}) \cdot \boldsymbol{u} \tag{86}$$

, where I introduced new knowledge vector $\boldsymbol{y} = \boldsymbol{O^T} \cdot \boldsymbol{z}$, and new state vector $\boldsymbol{u} = \boldsymbol{O^T} \cdot \boldsymbol{x}$. Vector $\boldsymbol{u}$ is the state vector represented in *eigenbasis* of the measuring device. Action of $exp(\boldsymbol{D^T})$ operator on vector $\boldsymbol{u}$ in (86) constitutes transformation by the measuring device. I define *eigenspaces* of the measuring device as *2D* subspaces formed by pairs of eigenvectors corresponding to eigenvalues $\pm\varphi_k$ in (83). In eigenbasis, the action of the measuring device is reduced to rotations in *2D* orthogonal *eigenspaces*, as evident from (85).

As I mentioned earlier, the rank of matrices $\boldsymbol{D}$, $\boldsymbol{O}$ and of vectors $\boldsymbol{x}, \boldsymbol{z}, \boldsymbol{y}, \boldsymbol{u}$ is $M-1$. Therefore, transformation (86) takes especially simple form in case of $M = 3$:

$$\boldsymbol{y} = \begin{pmatrix} y_1 \\ y_2 \end{pmatrix} = \begin{pmatrix} cos(\varphi) & -sin(\varphi) \\ sin(\varphi) & cos(\varphi) \end{pmatrix} \cdot \boldsymbol{u} \text{ , where } \varphi = \varphi(t, \boldsymbol{u}) \text{ , and } \boldsymbol{u} = \begin{pmatrix} u_1 \\ u_2 \end{pmatrix} \tag{87}$$

When $M = \{1, 2\}$ the transformation is trivial: if $M = 1$ then $\boldsymbol{y} \equiv 0$; if $M = 2$ then $\boldsymbol{y} = 1 \cdot \boldsymbol{u}$. Transformation (87) can be expressed in complex notation using real components $u_1, u_{2,} y_1, y_2$:

$$\boldsymbol{y} = \begin{pmatrix} e^{i\varphi} & 0 \\ 0 & e^{-i\varphi} \end{pmatrix} \cdot \boldsymbol{u} \text{ , where } \boldsymbol{u} = \frac{1}{\sqrt{2}} \cdot \begin{pmatrix} u_1 + iu_2 \\ u_1 - iu_2 \end{pmatrix} \text{ , and } \boldsymbol{y} = \frac{1}{\sqrt{2}} \cdot \begin{pmatrix} y_1 + iy_2 \\ y_1 - iy_2 \end{pmatrix} \tag{88}$$

In case of $M > 3$ one can convert to complex notation by combining pairs of real $\{u_k\}$, $\{y_k\}$ components corresponding to *2D* eigenspaces in (85) into complex numbers as in (88). In case of even M there will be one real-only component u_i left un-transformed. In complex notation, (85) can be written as a Lie group $SU(M-1)$ unitary matrix $\boldsymbol{U}$:

for even M: $$\boldsymbol{U} = \begin{pmatrix} 1 & & & & & \\ & \boldsymbol{e}^{-i\varphi_1} & & \cdots & 0 & \\ & & \boldsymbol{e}^{i\varphi_1} & & & \\ & \vdots & & \ddots & \vdots & \\ & 0 & & \cdots & \boldsymbol{e}^{-i\varphi_n} & \\ & & & & & \boldsymbol{e}^{i\varphi_n} \end{pmatrix} \quad \text{, where} \quad \varphi_k = \varphi_k(t, \boldsymbol{u}) \tag{89}$$

, and for odd M: $$\boldsymbol{U} = \begin{pmatrix} \boldsymbol{e}^{-i\varphi_1} & & & & \\ & \boldsymbol{e}^{i\varphi_1} & \cdots & 0 & \\ \vdots & & \ddots & \vdots & \\ 0 & & \cdots & \boldsymbol{e}^{-i\varphi_n} & \\ & & & & \boldsymbol{e}^{i\varphi_n} \end{pmatrix} \tag{90}$$

Transformation (86) can now be expressed in complex notation as:

$$\boldsymbol{y} = \boldsymbol{U}^{\dagger} \cdot \boldsymbol{u} \tag{91}$$

In complex notation, $SO(M-1)$ matrix (85) takes diagonal form and becomes $SU(M-1)$ matrix (89-90). Operating with unitary matrices in diagonal form is easier than with orthogonal matrix (85). The complex notation is a technique to make some math easier to handle, not to create new physics out of thin air.

Consider scenario where eigenspaces of the measuring device do not depend on time or on the state vector of underlying system, i.e. $\partial \boldsymbol{O}/\partial t = 0$ in (86). That deems a valid expectation if measuring device is to provide consistent results. It means, e.g., the orientation of polarizer does not depend on time, or on the polarization of incident light. Then, from (27), $\langle \partial \boldsymbol{u}/\partial t \rangle = 0$. Assuming analytic $\varphi_k(t, \boldsymbol{u})$:

$$\langle \frac{\partial \boldsymbol{y}}{\partial t} \rangle = \langle \frac{\partial}{\partial t} (\boldsymbol{U}^{\dagger} \boldsymbol{u}) \rangle = i \cdot \boldsymbol{\Phi}^{\dagger} \cdot \boldsymbol{y} \tag{92}$$

, where, for even M:

$$\boldsymbol{\Phi} = \begin{pmatrix} 0 & & & & & \\ & \theta_1 & & \cdots & 0 & \\ & & -\theta_1 & & & \\ & \vdots & & \ddots & \vdots & \\ & 0 & & \cdots & \theta_n & \\ & & & & & -\theta_n \end{pmatrix} \tag{93}$$

, and for odd M:

$$\boldsymbol{\Phi} = \begin{pmatrix} \theta_1 & & & & \\ & -\theta_1 & \cdots & 0 & \\ \vdots & & \ddots & \vdots & \\ 0 & & \cdots & \theta_n & \\ & & & & -\theta_n \end{pmatrix} \tag{94}$$

, where $$\theta_k = \frac{\partial \varphi_k(t, \boldsymbol{u})}{\partial t} \tag{95}$$

If eigenspace component $\boldsymbol{u}_k = 0$, the underlying system is in a state characterized by the symmetry with respect to rotations within k^{th} *2D* eigenspace of the measuring device. Therefore, the eigenspace component $\boldsymbol{y}_k$ will not rotate if $\boldsymbol{u}_k = 0$, i.e. *null vector has no phase*. Thus, $\theta_k(\boldsymbol{u}_k = 0) = 0$. In the vicinity of $\boldsymbol{u}_k = 0$, $\theta_k(\boldsymbol{u})$ is approximated by a positive quadratic form on $\boldsymbol{u}_k$. The only such form is the eigenspace component of energy:

$$\theta_k = \frac{\mathcal{E}_k}{\hbar} \quad \text{, where} \quad \mathcal{E}_k = \frac{\langle u_k | u_k \rangle}{2N} = \frac{\langle y_k | y_k \rangle}{2N} \quad \text{, and} \quad \sum_k \mathcal{E}_k = \mathcal{E} \tag{96}$$

, and $\hbar$ is a constant of proportionality which I'm tempted to call Planck's constant. No model is complete if it contains underived physical constants. To obtain an expression for $\hbar$, I note that in a case of $N = 1$ and $M = 3$, there are 3 canonical vectors possible, from (22):

$$\begin{pmatrix} -1/\sqrt{2} \\ \sqrt{3/2} \end{pmatrix}, \begin{pmatrix} -1/\sqrt{2} \\ -\sqrt{3/2} \end{pmatrix}, \begin{pmatrix} \sqrt{2} \\ 0 \end{pmatrix} \tag{97}$$

The phase difference between these vectors is $2\pi/3$. Thus, for underlying system with $N = 1$ and $M = 3$, the proper time (1) increment $\tau = \Delta(\ln N) = 1/N$ corresponds to a phase increment $\Delta\varphi = 2\pi/3$. The energy (9) of underlying system with $N = 1$ and $M = 3$ is $\mathcal{E} = -3 \cdot \ln \Gamma(4/3) \cong 1/3$. Thus, in proper time scale of the system with $N = 1$, the value of the Planck's constant is:

$$\hbar = \frac{\mathcal{E} \cdot \tau}{\Delta\varphi} \cong \frac{1}{2\pi} \qquad ; \qquad h = 2\pi\hbar = 1 \tag{98}$$

A classical measuring device, such as the wall clock, is coupled into environment via various interactions, electromagnetic, gravitational, etc. Effectively, it is part of the whole universe. Its proper time is the universe' proper time, defined by the total population number (1) of microstates in statistical ensemble representing the universe. In universe' proper time scale (98) becomes:

$$\hbar \cong \frac{1}{2\pi N} \qquad ; \qquad h = 2\pi\hbar = 1/N \tag{99}$$

From (99) it follows, the Planck's constant ought to decrease with time $t = \ln N$. Although, given the number N is likely to be very large, the decrease $\Delta\hbar/\hbar = -\Delta N/N$ might not be detectable. Since the time increments $\tau = 1/N$ also decrease, the product $\Delta\varphi = \mathcal{E} \cdot \tau/\hbar$ stays the same. The decrease in the value of $\hbar$ is negated by the slowing time. It is not clear if such decrease can be detected at all given all measurements of Planck's constant [35], in effect, are measurements of the product $\hbar\omega$ or $\Delta\mathcal{E} \cdot \tau/\hbar$. The dimensionless value (99) of Planck's constant does not expound the observable timescales, which are to be determined from empirical evidence.

Unlike (91), the equation (92) with (93-95) only contains reference to knowledge vector $\boldsymbol{y}$, and no reference to the state vector $\boldsymbol{u}$ of underlying system. The linearity of (92) means the *expected* past and the future of knowledge vector are unambiguously defined *in the present*. The expectation that the current state contains information about the past gives rise to the concept of *memory*. The *past* or the *future* are the knowledge vectors defined in the *present* and related by transformation:

$$\boldsymbol{U} = exp\big(-i\boldsymbol{\Phi} \cdot (t - t_0)\big) \tag{100}$$

The measurement device performing transformation (100) maintains phase relationship (coherence) between knowledge vectors. I call it a *quantum device*.

Equation (92) is similar to Schrödinger equation where $\boldsymbol{H}$-matrix $= -\hbar\boldsymbol{\Phi}$, and where θ_i are the characteristic frequencies. The notable difference is that (92) incorporates measurement apparatus, as it describes the *expected* evolution of knowledge vector as rotations within *2D* eigenspaces of the measuring device. The Schrödinger equation describes evolution of wave function as if it exists as some sort of physical reality outside of measurement apparatus. Schrödinger himself believed wave function is a physical reality, a density wave [36]. It is rather common in physics community [37], and others (see e.g. Tangled up in Entanglement by L.M. Krauss and response by D. Chopra) to assume the evolution of wave function according to Schrödinger equation is independent of the observer, i.e. independent of *representation*.

The expectation of the equivalence of different representations is born out of assumption of *realism*, i.e. of observed system existing and possessing properties independent of observer. If different representations are not equivalent, physicists are confronted with the choice of *preferred basis* [14]. The assumption of realism led to a number of theories alternative to *Copenhagen*

Interpretation, such as *many worlds* [38] and *pilot wave* [39]. The Copenhagen Interpretation maintains underlying system does not have definite properties prior to being measured. In different representations, objects may demonstrate contradictory behavior, as in interference experiments [15] where objects behave either as waves, or as classical particles depending on configuration of measuring apparatus. If device maintains phase relationship between knowledge vectors, the observed object exhibits wave-like behavior. Without phase relationship between knowledge vectors, classical behavior is observed, as I show below. The corresponding experimental setups provide examples of [unitarily] non-equivalent representations. It is trivial to prove there could be no unitary transformation from quantum to a classical behavior. Consider a system in a pure quantum state. Its density matrix $\boldsymbol{\rho}$ satisfies $\boldsymbol{\rho}^2 = \boldsymbol{\rho}$. If unitary transformation $\boldsymbol{U}$, such as time propagator $\boldsymbol{U} = exp(i\boldsymbol{H} \cdot t/\hbar)$, is applied to $\boldsymbol{\rho}$, then density matrix $\boldsymbol{q}$ in the new basis is $\boldsymbol{q} = \boldsymbol{U}\boldsymbol{\rho}\boldsymbol{U}^{\dagger}$. It is easy to see that $\boldsymbol{q}^2 = \boldsymbol{q}$, i.e. the system remains in a pure quantum state. It will also be true in case of time-dependent $\boldsymbol{H}(t)$, i.e. no [coherent] coupling of external fields can force a pure quantum system to transform into a classical, or a mixed state. The existence of non-equivalent representations has been proven by Haag [40] but its significance is still not fully appreciated.

The measurement result is [usually] a finite scalar value. It's natural to assume it is an analytic scalar function $J(\boldsymbol{y})$ of knowledge vector $\boldsymbol{y}$ with minimum at $J(\boldsymbol{y} = 0)$=0. Due to above-mentioned symmetry of $\boldsymbol{u}_k = 0$ state, in the vicinity of $\boldsymbol{y} = 0$, $J(\boldsymbol{y})$ is approximated by a positive semi-definite quadratic form on $\boldsymbol{y}$, diagonal in device eigenbasis:

$$J(\boldsymbol{y}) = \frac{\langle \boldsymbol{y}|\boldsymbol{F}|\boldsymbol{y}\rangle}{2N} = \sum_k f_k \cdot \mathcal{E}_k \tag{101}$$

, where index k spans eigenspaces of the measuring device; $\boldsymbol{F}$ is the operator matrix of observable; f_k are eigenvalues of $\boldsymbol{F}$; $\mathcal{E}_k$ are eigenspace components of energy (96); f_k are device calibration constants. For any observable, there exists a device eigenbasis in which the operator matrix $\boldsymbol{F}$ of the observable is diagonal. In real number notation, matrix $\boldsymbol{F}$ must be positive semi-definite in order for the *observed values* f_k to be real non-negative numbers. In complex notation (91), the eigenvalues of $\boldsymbol{F}$ come in complex-conjugate pairs. In this case f_k in (101) is the real part of the eigenvalue. In canonical basis (22), the device is defined by a symmetric matrix $\boldsymbol{F}' = \boldsymbol{O}\boldsymbol{F}\boldsymbol{O}^{\boldsymbol{T}}$, where matrix $\boldsymbol{O}$ defines eigenspaces, as in (85), and diagonal matrix $\boldsymbol{F}$ defines eigenvalues.

The quadratic form approximation is invalid under higher energies. However, the rightmost side of (101) is expressed in terms of energy eigenspace components, not as a quadratic form on knowledge vector. It is conceivable the rightmost side of (101) is not an approximation. It may be valid for the whole range of energy values, including region of higher energies, where linear dependence of $\mathcal{E}$ on quantum number breaks down (Figure 1).

If operator matrix of observable $\boldsymbol{A}$ is diagonal in eigenbasis of device $\boldsymbol{U}_1$, and operator matrix of observable $\boldsymbol{B}$ is diagonal in eigenbasis of device $\boldsymbol{U}_2$, and if devices $\boldsymbol{U}_1$ and $\boldsymbol{U}_2$ have different eigenspaces, then matrices $\boldsymbol{A}$ and $\boldsymbol{B}$ do not commute. Hence, the generalized uncertainty principle [21] applies if observables $\boldsymbol{A}$ and $\boldsymbol{B}$ are measured in eigenbasis $\boldsymbol{y}$ of some third device $\boldsymbol{U}_3$:

$$\sigma_{\boldsymbol{A}}^2 \cdot \sigma_{\boldsymbol{B}}^2 \geq \frac{1}{4}|\langle \boldsymbol{y}|\boldsymbol{A}\boldsymbol{B} - \boldsymbol{B}\boldsymbol{A}|\boldsymbol{y}\rangle|^2 \tag{102}$$

The canonical state vector $\boldsymbol{x}$ can be expressed as a sum (26) of canonical state vectors. Similar decomposition $\boldsymbol{y} = \sum \boldsymbol{y}_i$ of the knowledge vector can be used for input to quadratic form (101):

$$J(\boldsymbol{y}) = \sum_{\boldsymbol{a},\boldsymbol{b}\in\{\boldsymbol{y}_i\}} \frac{\langle \boldsymbol{a}|\boldsymbol{F}|\boldsymbol{b}\rangle}{2N} = \sum_k f_k \cdot \sum_{\boldsymbol{a},\boldsymbol{b}\in\{\boldsymbol{y}_i\}} r_{\boldsymbol{a}_k} \cdot r_{\boldsymbol{b}_k} \cdot \cos\left(\varphi_{\boldsymbol{a}_k} - \varphi_{\boldsymbol{b}_k}\right) \tag{103}$$

, where $\varphi_{\boldsymbol{a}_k}$; $\varphi_{\boldsymbol{b}_k}$ are k^{th} eigenspace phases (89) of vectors $\boldsymbol{a}, \boldsymbol{b} \in \{\boldsymbol{y}_i\}$; $r_{\boldsymbol{a}_k} = \left[N_a \mathcal{E}_{\boldsymbol{a}_k}/N\right]^{1/2}$; $\mathcal{E}_{\boldsymbol{a}_k} = \langle \boldsymbol{a}_k | \boldsymbol{a}_k \rangle / (2N_a)$. The decomposition $\boldsymbol{y} = \sum \boldsymbol{y}_i$ is selected from possible decompositions of $\boldsymbol{y}$ by the measuring device, through entanglement with underlying system. Device acts as a filter, only entangling with modes $\{\boldsymbol{u_i}\}$ which match device modes. In device eigenbasis, such modes are the knowledge vectors $\{\boldsymbol{y}_i\}$. I will also call them medium oscillators.

Depending on the context, knowledge vectors $\boldsymbol{a}, \boldsymbol{b} \in \{\boldsymbol{y}_i\}$ in (103) may bear different meaning. In time-correlation measurement, vector $\boldsymbol{b}$ is viewed as state vector *before-transition*, and vector $\boldsymbol{a}$ – as *after-transition*. In case of spatial correlation, vector $\boldsymbol{a}$ may be viewed as observer *Alice*, and vector $\boldsymbol{b}$ – as observer *Bob*. The expression (103) simplifies for $M = 3$, with $f = 1$:

$$J(\boldsymbol{y}) = \sum_{\boldsymbol{a},\boldsymbol{b} \in \{\boldsymbol{y}_i\}} r_{\boldsymbol{a}} \cdot r_{\boldsymbol{b}} \cdot \cos(\varphi_{\boldsymbol{a}} - \varphi_{\boldsymbol{b}}) \quad \text{, where} \quad r_{\boldsymbol{a}} = \sqrt{N_{\boldsymbol{a}} \mathcal{E}_{\boldsymbol{a}}/N} \tag{104}$$

The variance of the measurement scalar (104) is:

$$\sigma_J^2 = \sum_{(\boldsymbol{a} \neq \boldsymbol{b}) \in \{\boldsymbol{y}_i\}} r_{\boldsymbol{a}}^2 \, r_{\boldsymbol{b}}^2 \tag{105}$$

Signal (104) does not include transitions to $\mathcal{E}_{\boldsymbol{a}} = 0$ or from $\mathcal{E}_{\boldsymbol{b}} = 0$. Therefore, it is impossible to harvest *zero-point energy* or detect a zero-energy state with scalar measurement. A narrow-band device would have $N_{\boldsymbol{b}} \cong N_{\boldsymbol{a}} \cong N/K \;\; \forall \, \boldsymbol{a}, \boldsymbol{b} \in \{\boldsymbol{y}_i\}$, where K is the number of knowledge vectors in superposition $\boldsymbol{y} = \sum \boldsymbol{y}_i$. If a single transition does not change significantly the energy $\mathcal{E}_{\boldsymbol{a}}$ of a given mode, I can also assume $\mathcal{E}_{\boldsymbol{b}} \cong \mathcal{E}_{\boldsymbol{a}} \cong \mathcal{E} \; \forall \, \boldsymbol{a}, \boldsymbol{b} \in \{\boldsymbol{y}_i\}$, with $|\Delta\mathcal{E}|_{\boldsymbol{ab}} = |\mathcal{E}_{\boldsymbol{a}} - \mathcal{E}_{\boldsymbol{b}}| \ll \mathcal{E}$. These assumptions are equivalent to thermodynamic limit approximation. I then rewrite (104-105) as:

$$J(\boldsymbol{y}) = \frac{\mathcal{E}}{K} \cdot \sum_{\boldsymbol{a},\boldsymbol{b} \in \{\boldsymbol{y}_i\}} \cos(\varphi_{\boldsymbol{a}} - \varphi_{\boldsymbol{b}}) \tag{106}$$

$$\sigma_J^2 = \mathcal{E}^2 \cdot \left(1 - \frac{1}{K}\right) \tag{107}$$

Given $\varphi_{\boldsymbol{a}} = \varphi(\boldsymbol{a})$; $\varphi_{\boldsymbol{b}} = \varphi(\boldsymbol{b})$, I evaluate $\varphi_{\boldsymbol{a}} - \varphi_{\boldsymbol{b}}$ in (106) via linear expansion near initial values $\varphi(\boldsymbol{a}_0)$; $\varphi(\boldsymbol{b}_0)$:

$$\varphi_{\boldsymbol{a}} - \varphi_{\boldsymbol{b}} = \varphi(\boldsymbol{a}_0) - \varphi(\boldsymbol{b}_0) + \boldsymbol{\nabla}\varphi(\boldsymbol{a}) \cdot \Delta\boldsymbol{a} - \boldsymbol{\nabla}\varphi(\boldsymbol{b}) \cdot \Delta\boldsymbol{b} \tag{108}$$

In a case of temporal correlations, $\boldsymbol{a} = \boldsymbol{a}(t)$; $\boldsymbol{b} = \boldsymbol{b}(t)$. With (92-96), I rewrite (108) in the vicinity of initial state $[\boldsymbol{a}_0 = \boldsymbol{a}(t_0)] = [\boldsymbol{b}_0 = \boldsymbol{b}(t_0)]$ as:

$$\begin{aligned} \varphi_{\boldsymbol{a}} - \varphi_{\boldsymbol{b}} &= \varphi(\boldsymbol{a}_0) - \varphi(\boldsymbol{b}_0) + i\left[\langle \boldsymbol{\nabla}\varphi(\boldsymbol{a}) | \boldsymbol{\Phi}_{\boldsymbol{a}}^{\dagger} | \boldsymbol{a} \rangle - \langle \boldsymbol{\nabla}\varphi(\boldsymbol{b}) | \boldsymbol{\Phi}_{\boldsymbol{b}}^{\dagger} | \boldsymbol{b} \rangle\right] \cdot \tau \\ &= \left[\frac{a^*}{\langle \boldsymbol{a}|\boldsymbol{a} \rangle} \cdot \theta_{\boldsymbol{a}} \cdot a - \frac{b^*}{\langle \boldsymbol{b}|\boldsymbol{b} \rangle} \cdot \theta_{\boldsymbol{b}} \cdot b + c.c.\right] \cdot \tau = (\theta_{\boldsymbol{a}} - \theta_{\boldsymbol{b}}) \cdot \tau \\ &= (\mathcal{E}_{\boldsymbol{a}} - \mathcal{E}_{\boldsymbol{b}}) \cdot \tau/\hbar = \pm\omega_{ab} \cdot \tau \end{aligned} \tag{109}$$

, where $\tau = t - t_0$ is the transition time; $\boldsymbol{\nabla}\varphi(\boldsymbol{a})$ is the complex gradient of scalar phase:

$$\langle \boldsymbol{\nabla}\varphi(\boldsymbol{a})| = \left(\frac{\partial\varphi}{\partial a}, \frac{\partial\varphi}{\partial a^*}\right) = \frac{\langle \boldsymbol{a}|}{\langle \boldsymbol{a}|\boldsymbol{a} \rangle} \cdot \begin{pmatrix} -i & 0 \\ 0 & i \end{pmatrix} \quad \text{, where } \langle \boldsymbol{a}| = (a^*, a) \tag{110}$$

For a device to detect transition $\boldsymbol{b} \to \boldsymbol{a}$, signal $J(\boldsymbol{y})$ must vary more than its standard deviation σ_J. The detection fidelity is characterized by a change from statistical mean, expressed in terms of a number of standard deviations. In [41] the *half-life* threshold was used – the decrease of the signal by half from its initial value $J(\boldsymbol{y})|_{\boldsymbol{a}=\boldsymbol{b}}$. For superposition $\boldsymbol{y} = \boldsymbol{a} + \boldsymbol{b}$ in (106-107), it corresponds to $\Delta J = \sqrt{2} \cdot \sigma_J$. The detection fidelity in this case is $erf(1) \cong 0.84$, i.e. the probability the change ΔJ was due to transition is 84%, and probability that it happened due to statistical error is 16%. For $\boldsymbol{y} = \boldsymbol{a} + \boldsymbol{b}$; $K = 2$; from (106-107):

$$J(\boldsymbol{y}) = \mathcal{E} \cdot (1 + \cos(\varphi_{\boldsymbol{a}} - \varphi_{\boldsymbol{b}})) \tag{111}$$

$$\sigma_J^2 = \mathcal{E}^2/2 \tag{112}$$

Signal (111) decreases by half from its initial value $J|_{\boldsymbol{a}=\boldsymbol{b}} = 2\mathcal{E}$, when $|\varphi_{\boldsymbol{a}} - \varphi_{\boldsymbol{b}}| = \pi/2$. Therefore, the half-life detection threshold satisfies energy-time uncertainty relation in a form of Mandelstam-Tamm bound [42]:

$$|\varphi_{\boldsymbol{a}} - \varphi_{\boldsymbol{b}}| = |\Delta\mathcal{E}|_{ab} \cdot \tau/\hbar = \omega_{ab} \cdot \tau \geq \pi/2 \tag{113}$$

I call the superposition of knowledge vectors $\boldsymbol{a}$, $\boldsymbol{b}$ *coherent* within interval $t_0 \leq t < t_0 + \tau$, if the difference $\varphi_{\boldsymbol{a}} - \varphi_{\boldsymbol{b}}$ is an analytic function of t in the interval. I call $\partial \ln J/\partial t|_{t=t_0}$ the *transition rate*. For the coherent superposition of knowledge vectors, with $\boldsymbol{a}(t_0) = \boldsymbol{b}(t_0)$, the transition rate $\partial \ln J/\partial t|_{t=t_0} = 0$. This result is referred to as *Zeno paradox* [43]. It is the characteristic feature of measurement with quantum device.

The non-zero transition rate arises from de-coherence of knowledge vectors through random phase dispersion caused by various mechanisms, e.g. by:

1. Rayleigh scattering [44, 45]
2. Brownian motion [46, 47]
3. Dispersive media [48, 49]
4. Recombination of electron-hole pairs in semiconductors [50]

A transition changes energy (48) by $\Delta\mathcal{E} = \pm\hbar\omega$ with equal probability in either direction. The case of $\Delta\mathcal{E} = \pm n\hbar\omega$, where $n > 1$, is equivalent to n consecutive transitions in the same direction. I call device which undergoes multiple transitions at random within any given interval Δt a *classical device*. In time Δt the phases φ_i of knowledge vectors $\{\boldsymbol{y}_i\}$ in (106) undergo a number of positive and negative increments with equal probability $p = 1/2$. The resultant increments are binomially distributed with mean $\Delta t/(2\tau)$, and variance $\sigma^2 = p \cdot (1-p) \cdot \Delta t/\tau = \Delta t/(4\tau)$. Here, τ is the *mean free time* between transitions, i.e. *de-coherence* time. In between transitions, the phase difference $\varphi_{\boldsymbol{a}} - \varphi_{\boldsymbol{b}}$ changes according to (109). It gives rise to the variance in phase $\sigma_\varphi^2 = (\omega\tau)^2\sigma^2 = \omega^2\tau\Delta t/4$, and to the variance in phase difference $\sigma_{\Delta\varphi}^2 = 4\sigma_\varphi^2 = \omega^2\tau\Delta t$.

Figure 11 shows numeric calculation of (106), with binomially distributed phases $\varphi_{\{\boldsymbol{y}_i\}}$. The calculation established the following:

$$J(\boldsymbol{y}) = \mathcal{E} \cdot [1 + (K-1) \cdot exp(-\omega^2 \cdot \tau \cdot \Delta t)] \tag{114}$$

The exponential decay (114) is the characteristic feature of a classical process. From (114), the transition rate in $K \to \infty$ limit:

$$\left.\frac{\partial \ln J}{\partial t}\right|_{t=t_0} = -\left(1 - \frac{1}{K}\right) \cdot \omega^2 \cdot \tau = -\omega^2 \cdot \tau \tag{115}$$

The half-life threshold (113), in this case, changes to:

$$\omega^2\tau\Delta t \geq \ln 2 \qquad \text{, given} \qquad \tau \ll \Delta t \tag{116}$$

From (116), $\Delta t \sim \ln 2/(\omega^2\tau)$, where Δt is the object's *decay time*. The expression (116) establishes relation between *de-coherence* and *decay* times. Quantum de-coherence has received an extensive coverage in last decades. A link between de-coherence and decay has been suggested [51]. De-coherence between knowledge vectors is not unlike the spontaneous collapse of wave function, a subject of a number of collapse theories [52].

Consider a photodetector measuring intensity of incident radiation. A knowledge vector $\boldsymbol{y}_i$ (a medium oscillator) is formed when a set of elements (e.g. electron-hole pairs) on the surface of photodetector entangle through some medium, e.g. through electromagnetic field. An analog of such entanglement is a Cooper pair in superconductor, mediated by phonon interaction. The

surface area which encloses a set of elements in entangled state is limited by the coherence radius $r = 2\pi\, c/(\kappa\Delta\omega)$, where c is the speed of light, κ is the refractive index of the material. If ρ is the number of entangled elements per unit area of the detector; D_ω is the dimensionless *scattering rate*; $D_\omega \cdot \Delta\omega$ is the scattering frequency within $\Delta\omega$ [*rad/s*] spectral width, then, the de-coherence time τ is evaluated as:

$$\tau = (\pi r^2 \rho D_\omega \Delta\omega)^{-1} = \left(\pi \left(\frac{2\pi c}{\kappa\Delta\omega}\right)^2 \rho D_\omega \Delta\omega\right)^{-1} = \frac{\kappa^2}{4\pi^3 c^2 \rho D_\omega}\Delta\omega \tag{117}$$

Combining (117) with (115), I obtain transition rate:

$$\left.\frac{\partial \ln J}{\partial t}\right|_{t=t_0} = -\frac{\kappa^2 \omega^2 \Delta\omega}{4\pi^3 c^2 \rho D_\omega} \tag{118}$$

In equilibrium, the loss of a number of oscillators in a particular mode is compensated by the radiation-stimulated induction into the mode of the same number of oscillators. The energy balance equation is:

$$R_\omega \cdot B_\omega \cdot \Delta\omega + \xi \cdot \left[\langle \mathcal{E} \rangle_\omega - \frac{\hbar\omega}{2}\right] \cdot \left.\frac{\partial \ln J}{\partial t}\right|_{t=t_0} = 0 \tag{119}$$

, where B_ω is the spectral radiance of incident radiation; R_ω is the efficiency of conversion of the incident radiation into oscillator energy; ξ is the number of medium oscillators per unit surface area of the detector. I have to subtract zero-point energy term $\hbar\omega/2$ from the ensemble-average energy $\langle \mathcal{E} \rangle_\omega$ in (119), because an oscillator cannot lose energy in the ground state. From (79,119):

$$R_\omega \cdot B_\omega = \frac{\xi \cdot \kappa^2}{\rho \cdot D_\omega}\left[\frac{\hbar\omega^3/(4\pi^3 c^2)}{\exp\left(\frac{\hbar\omega}{kT}\right) - 1}\right] \tag{120}$$

The term in square brackets can be considered as pertaining to the incident radiation, and parameters outside the brackets as properties of the detector. Then, (120) can be split into formula for the spectral radiance, and formula for the detector efficiency:

$$B_\omega = \frac{\hbar\omega^3/(4\pi^3 c^2)}{\exp\left(\frac{\hbar\omega}{kT}\right) - 1} \tag{121}$$

$$R_\omega = \frac{\xi \cdot \kappa^2}{\rho \cdot D_\omega} = \frac{\kappa^2}{\eta \cdot D_\omega} \tag{122}$$

, where $\eta = \rho/\xi$ can be interpreted as the number of entangled elements making up one oscillator. The Planck's formula for the spectral energy density readily follows from (121):

$$u_\omega = \frac{4\pi}{c} B_\omega = \frac{\hbar\omega^3/(\pi^2 c^3)}{\exp\left(\frac{\hbar\omega}{kT}\right) - 1} \tag{123}$$

5. DISCUSSION

The presented model bears familiar hallmarks of quantum physics. Consider e.g. wave-particle duality. The particle properties result from discreteness of probability mass function (4), of energy spectrum (Table 1), of proper time (1), of measurement scalar (101,103,106). The discrete values of measurement scalar may be associated with observable states of underlying system. The choice of observation basis (i.e. the experimental setup) can make quantum leaps between observable values look like emission and absorption of particles.

Wave properties result from superposition $\boldsymbol{y} = \sum \boldsymbol{y}_i$ of knowledge vectors in the measurement scalar (103,106). The superposition should rather be called *decomposition*, as the knowledge vector $\boldsymbol{y}$ of underlying system is decomposed into a sum of eigenvectors $\{\boldsymbol{y}_i\}$ of the measuring device. For a simple case $\boldsymbol{y} = \boldsymbol{a} + \boldsymbol{b}$, the expression for the measurement scalar (111) is identical to the intensity distribution in interference pattern in a double-slit experiment.

Consider another QM hallmark: violation of Bell's inequalities [53]. The violation of Bell's inequalities can be understood without invoking the concept of wave function collapse. In a typical experiment [54, 55] two entangled particles represent the same underlying system, which is being observed via two spatially separated devices $\boldsymbol{A}$ and $\boldsymbol{B}$. An observer *Alice* is attached to device $\boldsymbol{A}$, and observer *Bob* is attached to device $\boldsymbol{B}$. If *Alice* and *Bob* did not communicate via conventional channel, neither of them would know the result of the other. The *statistical correlation* can only be detected when knowledge vectors $\boldsymbol{a}$ and $\boldsymbol{b}$ converge to form the resultant observation (111). The target of experiments on violation of Bell's inequalities is the $\cos()$ function in (111). It shows double-slit experiment is about as good experiment on violation of Bell's inequalities as any other. Confusion of statistical correlation with causality in this context led some minds to bewilderment about *spooky action at a distance* [56].

Consider the concept of measurement in conventional QM theory. If measurement $\boldsymbol{Q}(t)$ has been performed at time $t = 0$, and the result is q_0, the expectation value at time $t > 0$ is given by:

$$q(t) = \langle \boldsymbol{u}_0 | \boldsymbol{U}(t)\boldsymbol{Q}(0)\boldsymbol{U}^{\dagger}(t) | \boldsymbol{u}_0 \rangle \text{ , where } \quad \boldsymbol{U}(t) = exp\left(i\frac{\boldsymbol{H}}{\hbar}t\right); \ \boldsymbol{H} \text{ is Hamiltonian,} \tag{124}$$

, and $\boldsymbol{u}_0$ is the state of the system at $t = 0$. Is the system considered closed or open? Conventional theory would imply the system is closed, as only a closed system can be described by a state vector. If the system is closed, it has to be in energy eigenstate. If $\boldsymbol{u}_0$ is also an energy eigenstate, then from (124), $q(t) \equiv q_0 \ \forall \ t \geq 0$, i.e. a closed system ought to be static. The conventional theory handles this paradox by considering system quasi-closed, i.e. initially described by a state vector, but with $\boldsymbol{H}$-matrix having off-diagonal terms. Then $\boldsymbol{H}$ is not a true Hamiltonian of the system but so-called *interaction Hamiltonian*, and $\boldsymbol{u}_0$ is not an eigenstate of $\boldsymbol{H}$.

According to *Heisenberg picture* of QM formalism, the measurement $\boldsymbol{Q}(t) = \boldsymbol{U}(t)\boldsymbol{Q}(0)\boldsymbol{U}^{\dagger}(t)$ is obtained from measurement $\boldsymbol{Q}(t = 0)$ via unitary transformation $\boldsymbol{U}(t)$ of observation basis. Since the result of the measurement at $t = 0$ is one of the eigenvalues of operator $\boldsymbol{Q}(0)$, the state $\boldsymbol{u}_0$ of the system at $t = 0$ has to be one of the eigenstates of $\boldsymbol{Q}(0)$. Attempts to understand this fact have needlessly led *Copenhagen School* to the concept of *wave function collapse*. If $\boldsymbol{u}_s$ are eigenvectors of $\boldsymbol{Q}(0)$, corresponding to eigenvalues q_s, then

$$\boldsymbol{Q}(0) = \sum_s |\boldsymbol{u}_s\rangle q_s \langle \boldsymbol{u}_s| = \sum_{s,j,k} |\boldsymbol{f}_j\rangle\langle \boldsymbol{f}_j|\boldsymbol{u}_s\rangle q_s \langle \boldsymbol{u}_s|\boldsymbol{f}_k\rangle\langle \boldsymbol{f}_k| \tag{125}$$

, where I converted to eigenbasis $\boldsymbol{f}_k$ of $\boldsymbol{H}$-matrix. It allows rewriting (125) as

$$q(t) = \sum_{s,j,k} \langle \boldsymbol{u}_0|\boldsymbol{f}_j\rangle \langle \boldsymbol{f}_j|\boldsymbol{u}_s\rangle q_s \langle \boldsymbol{u}_s|\boldsymbol{f}_k\rangle\langle \boldsymbol{f}_k|\boldsymbol{u}_0\rangle \cdot exp\left(i\frac{E_j - E_k}{\hbar}t\right) \tag{126}$$

, where E_j are eigenvalues of $\boldsymbol{H}$. Coefficients $\langle \boldsymbol{u}_0|\boldsymbol{f}_j\rangle\langle \boldsymbol{f}_j|\boldsymbol{u}_s\rangle q_s \langle \boldsymbol{u}_s|\boldsymbol{f}_k\rangle\langle \boldsymbol{f}_k|\boldsymbol{u}_0\rangle$ are all real because their transpose by j, k indices is equal to their adjoint. Hence, I rewrite (126) as:

$$q(t) = \sum_{s,j,k} \langle \boldsymbol{u}_0|\boldsymbol{f}_j\rangle\langle \boldsymbol{f}_j|\boldsymbol{u}_s\rangle q_s \langle \boldsymbol{u}_s|\boldsymbol{f}_k\rangle\langle \boldsymbol{f}_k|\boldsymbol{u}_0\rangle \cdot cos\left(\frac{E_j - E_k}{\hbar}t\right) \tag{127}$$

From (127) it is clear that $\big(q(0) - q(t)\big)|_{t\to 0} \propto t^2$ [43, 57], which can also be demonstrated if (127) is broken into power series of t near $t = 0$:

$$q(t) = \left\langle \boldsymbol{u}_0 \middle| cos\left(ad\left(\frac{\boldsymbol{H}}{\hbar}t\right)\right)\boldsymbol{Q} \middle| \boldsymbol{u}_0 \right\rangle = q_0 - \frac{t^2}{2\hbar^2}\langle \boldsymbol{u}_0 | [\boldsymbol{H},[\boldsymbol{H},\boldsymbol{Q}]] | \boldsymbol{u}_0 \rangle + \frac{t^4}{24\hbar^4}\left\langle \boldsymbol{u}_0 \middle| \left[\boldsymbol{H},\left[\boldsymbol{H},[\boldsymbol{H},[\boldsymbol{H},\boldsymbol{Q}]]\right]\right] \middle| \boldsymbol{u}_0 \right\rangle + o(t^6) \tag{128}$$

, where $ad(\boldsymbol{H})\boldsymbol{Q} = [\boldsymbol{H},\boldsymbol{Q}] = \boldsymbol{HQ} - \boldsymbol{QH}$ are commutator brackets. If the system was in state $\boldsymbol{u}_0$ at $t = 0$ then the probability $P(t)$ to find it in state $\boldsymbol{u}_0$ at $t > 0$ is:

$$P(t) = \sum_{j,k} P_j P_k \cdot cos\left(\frac{E_j - E_k}{\hbar}t\right) \quad \text{, where} \quad P_k = |\langle \boldsymbol{f}_k | \boldsymbol{u}_0 \rangle|^2 \tag{129}$$

From (127-129) it follows that $\partial q(t)/\partial t\,|_{t=0} = 0$; $\partial P(t)/\partial t\,|_{t=0} = 0$ leading to what is perceived as *quantum Zeno effect*.

The eigenvalues E_j of $\boldsymbol{H}$-matrix are not true energy levels of the system because $\boldsymbol{H}$-matrix is not a true Hamiltonian. They can also be defined up to an arbitrary constant, as only the difference $E_j - E_k$ matters for the dynamics of the system. The subtraction of a constant from eigenvalues of $\boldsymbol{H}$-matrix in (127-129) doesn't change the expectation value $q(t)$. Such technique is called re-normalization. The re-normalization [31] is used in conventional theory to "resolve" various ultraviolet catastrophes, including problem of infinite zero-point energy density resulting from $\hbar\omega/2$ term in (79). The problem with that approach is that $\hbar\omega$ term in (48,79) already refers to the difference between energy levels. Therefore, renormalization cannot possibly help here. Other problem with conventional theory is that it does not comply with Second Law of Thermodynamics (SLT), as Neumann's entropy [58] is invariant under unitary transformations. The SLT trumps any other law in physics, so any theory or model which is not compliant with SLT is faulty.

In the presented model, the canonical state vector (22) of underlying system has an associated value of time (1). The multiple possible histories of underlying system are represented by the sequences of statistical ensembles (n_i) arranged by time progression rule (2,3). The progression rule (2,3) results in increase of entropy (77) with time. In thermodynamic limit, the time progression of underlying system is approximated by rather featureless exponential decline (27). The observational diversity is rooted not in dynamics of underlying system, but in the dynamics (91-92) of observation basis.

This work has been motivated, in part, by:

- a perception of a common mechanism which might account for similar traits in vastly different entities
- an apprehension that modern science mostly operates within confinement of a *primitive realism*, which presents the world as a collection of solids of various shapes, liquids, gases, and progressively more exotic objects, all the way to the not quite defined notions of dark energy and dark matter, purported to make up 95% of the "reality"; with all those things existing somewhere "out there" beyond the tip of our noses
- a sense of contradiction between assumption of causal relationships which modern physics strives to establish, and probabilistic nature of observation outcome, implying there is no such thing as causality, just correlation

References

[1] W. Wislicki, "Thermodynamics of systems of finite sequences," *J. Phys. A: Math. Gen.*, vol. 23, no. 3, p. L121, 1990.

[2] C. Frenzen, "Explicit mean energies for the thermodynamics of systems of finite sequences," *J. Phys. A: Math. Gen.*, vol. 26, no. 9, p. 2269, 1993.

[3] S. Viznyuk, "Thermodynamic properties of finite binary strings," *arXiv:1001.4267 [cs.IT]*, 2010.

[4] R. Albert and A.-L. Barabási, "Statistical mechanics of complex networks," *Rev. Mod. Phys.*, vol. 74, pp. 47-97, 2002.

[5] G. Bianconi and A.-L. Barabási, "Bose-Einstein condensation in complex networks," *arXiv:cond-mat/0011224 [cond-mat.dis-nn]*, 2000.

[6] A.-L. Barabási and E. Bonabeau, "Scale-Free Networks," *Scientific American*, vol. 288, pp. 50-59, 2003.

[7] M. Bouchaud, "Wealth Condensation in a simple model of economy," *Physica A Statistical Mechanics and its Applications*, vol. 282, p. 536, 2000.

[8] T. Garrett, "Thermodynamics of long-run economic innovation and growth," *arXiv:1306.3554 [q-fin.GN]*, 2013.

[9] S. Sieniutycz and P. Salamon, Finite-Time Thermodynamics and Thermoeconomics, Taylor & Francis, 1990.

[10] J. Chan, T. Alegre, A. Safavi-Naeini, J. Hill, A. Krause, S. Groeblacher, M. Aspelmeyer and O. Painter, "Laser cooling of a nanomechanical oscillator into its quantum ground state," *arXiv:1106.3614 [quant-ph]*, 06 2011.

[11] R. Penrose, "On Gravity's Role in Quantum State Reduction," *General Relativity and Gravitation*, vol. 28, no. 5, pp. 581-600, 1996.

[12] A. Bassi and G. Ghirardi, "Dynamical Reduction Models," *arXiv:quant-ph/0302164*, 04 2003.

[13] S. Viznyuk, "Time as a parameter of statistical ensemble," *arXiv:1110.3296 [physics.gen-ph]*, 2011.

[14] T. Wang and D. Hobill, "Is the Preferred Basis selected by the environment?," *arXiv:1412.2852 [quant-ph]*, 2014.

[15] X.-s. Ma, J. Kofler and A. Zeilinger, "Delayed-choice gedanken experiments and their realizations," *arXiv:1407.2930v3 [quant-ph]*., 2016.

[16] C. Shannon, "A Mathematical Theory of Communication," *The Bell System Technical Journal*, vol. 27, pp. 379-423, 623-656, 1948.

[17] S. Viznyuk, "Shannon's entropy revisited," *arXiv:1504.01407 [cs.IT]*, 03 2015.

[18] K. Yamanaka, S. Kawano and K. Y., "Constant Time Generation of Integer Partitions," *IEICE Transactions on Fundamentals of Electronics, Communications and Computer Sciences*, Vols. E90-A, no. 5, pp. 888-895, 2007.

[19] S. Viznyuk, "OEIS sequence A210237," 2012. [Online]. Available: https://oeis.org/A210237. [Accessed 21 04 2015].

[20] C. Forbes, M. Evans, N. Hastings and B. Peacock, Statistical Distributions, Fourth Edition, Hoboken, NJ, USA: John Wiley & Sons, Inc., 2010.

[21] D. J. Griffiths, Introduction to Quantum Mechanics, 2nd ed., Pearson Education, Inc., 2005.

[22] N. Sloane, "OEIS sequence A003136," 1991. [Online]. Available: https://oeis.org/A003136. [Accessed 2015].

[23] I. Vapnyarskii, "Lagrange multipliers," in *Encyclopedia of Mathematics*, Springer, 2001.

[24] K. Huang, Introduction to Statistical Physics, Taylor & Francis, Inc., 2001.

[25] M. S. I. A. Abramowitz, "6.3 psi (Digamma) Function," in *Handbook of Mathematical Functions with Formulas, Graphs, and Mathematical Tables*, New York: Dover, 1972, p. 258–259.

[26] L. Landau and E. Lifshitz, Statistical Physics, vol. 5, Elmsford: Pergamon Press, Ltd., 1980.

[27] R. Evans, J. Boersma, N. M. Blachman and A. Jagers, "The Entropy of a Poisson Distribution: Problem 87-6," *SIAM Review,* vol. 30, no. 2, p. 314–317, 1988.

[28] K. Huang, Statistical Mechanics, John Wiley & Sons, 1987.

[29] "Planck's law," [Online]. Available: https://en.wikipedia.org/wiki/Planck%27s_law. [Accessed 20 06 2015].

[30] C. Kittel and H. Kroemer, Themal physics, W. H. Freeman, 1980.

[31] P. Jordan and W. Pauli, "Zur Quantenelektrodynamik ladungsfreier Felder," *Zeitschrift für Physik,* vol. 47, no. 3, pp. 151-173, 1928.

[32] G. Grundler, "The zero-point energy of elementary quantum fields," *arXiv:1711.03877 [physics.gen-ph],* Novermber 2017.

[33] D. Youla, "A normal form for a matrix under the unitary congruence group," *Canad. J. Math,* vol. 13, pp. 694-704, 1961.

[34] T. Voronov, "Pfaffian," in *Concise Encyclopedia of Supersymmetry*, Springer Netherlands, 2003, pp. 298-298.

[35] R. Steiner, "History and progress on accurate measurements of the Planck constant," *Reports on Progress in Physics,* vol. 76, no. 1, 2012.

[36] J. Bell, "Against 'measurement'," *Physics World,* August 1990.

[37] N. Mermin, "The Ithaca Interpretation of Quantum Mechanics," *arXiv:quant-ph/9609013,* 17 09 1996.

[38] B. S. DeWitt, "Quantum mechanics and reality," *Physics Today,* pp. 30-35, 1970.

[39] D. Bohm, "A suggested interpretation of the quantum theory in terms of hidden variables," *Phys. Rev.,* vol. 85, pp. 166-179, 1952.

[40] R. Haag, "On Quantum Field Theories," *Dan. Mat. Fys. Medd.,* vol. 29, no. 12, pp. 1-37, 1955.

[41] L. Mandelstam and I. Tamm, "The uncertainty relation between energy and time in non-relativistic quantum mechanics," *Journal of Physics,* vol. 9, no. 4, pp. 249-254, 1945.

[42] S. Deffner and S. Campbell, "Quantum speed limits: from Heisenberg's uncertainty principle to optimal quantum control," *arXiv:1705.08023 [quant-ph],* 16 10 2017.

[43] S. E. Misra B., "The Zeno's paradox in quantum theory," *Journal of Mathematical Physics,* vol. 18, no. 4, pp. 756-763, 1977.

[44] H. Uys, M. Biercuk, A. VanDevender, C. Ospelkaus, D. Meiser, R. Ozeri and J. Bollinger, "Decoherence due to Elastic Rayleigh Scattering," *Phys.Rev.Letters,* vol. 105, p. 200401, 2010.

[45] M. Schlosshauer, Decoherence and the quantum-to-classical transition, Springer, 2007.

[46] J. Paz, "Decoherence in Quantum Brownian Motion," *arXiv:gr-qc/9402007,* 02 1994.

[47] K. Hornberger, "Introduction to Decoherence Theory," *Lect. Notes Phys.,* pp. 221-276, 2009.

[48] C. Antonelli and e. al, "Sudden Death of Entanglement Induced by Polarization Mode Dispersion," *Phys.Rev.Letters,* vol. 106, no. 8, p. 080404, 02 2011.

[49] S. Salemian and S. Mohammadnejad, "Analysis of Polarisation Mode Dispersion Effect on Quantum State Decoherence in Fiber-based Optical Quantum Communication," in *Proceedings of the 2011 11th International Conference on Telecommunications (ConTEL),* Graz, 2011.

[50] Y. Jho, X. Wang, D. Reitze, J. Kono, A. Belyanin, V. Kocharovsky and G. Solomon, "Cooperative recombination of electron-hole pairs in semiconductor quantum wells under quantizing magnetic fields," *Phys.Rev. B,* vol. 81, pp. 155314-1, 2010.

[51] S. Viznyuk, "Gravity-induced decay," 2016. [Online]. Available: https://www.academia.edu/21674738/Gravity-induced_decay.

[52] G. Ghirardi, "Collapse Theories," 2016. [Online]. Available: https://plato.stanford.edu/entries/qm-collapse/.

[53] J. Bell, "On the Einstein Podolsky Rosen Paradox," *Physics,* vol. 1, no. 3, pp. 195-200, 1964.

[54] A. Aspect, P. Grangier and G. Roger, "Experimental Tests of Realistic Local Theories via Bell's Theorem," *Physical Review Letters,* vol. 47, no. 7, pp. 460-463, 1981.

[55] B. Hensen, H. Bernien, A. Dreau and e. all, "Loophole-free Bell inequality violation using electron spins separated by 1.3 kilometres," *Nature,* vol. 526, no. 686, October 2015.

[56] A. Einstein, N. Rosen and B. Podolsky, "Can Quantum-Mechanical Description of Physical Reality Be Considered Complete," *Phys. Rev.,* vol. 47, p. 777, 1935.

[57] S. A. Koshino K., "Quantum Zeno effect by general measurements," *arXiv:quant-ph/0411145,* 3 2005.

[58] J. Von Neumann, Mathematical Foundations of Quantum Mechanics, Princeton University Press, 1955.

[59] "Digamma function," [Online]. Available: http://en.wikipedia.org/wiki/Digamma_function. [Accessed 21 04 2015].

[60] S. J. Strickler, "Electronic Partition Function Paradox," *Journal of Chemical Education,* vol. 43, no. 7, pp. 364-366, 1966.

[61] S. Viznyuk, "Condensation into ground state in binary string models," *arXiv:1012.5318 [cs.IT],* 2010.

[62] D. Ward and S. Volkmer, "How to Derive the Schrodinger Equation," *arXiv:physics/0610121 [physics.hist-ph],* 2006.

[63] L. Kish, "Zero-point energy in the Johnson noise of resistors: Is it there?," *arXiv:1504.08229 [physics.gen-ph]*, 2015.

[64] "Unitary matrix," [Online]. Available: https://en.wikipedia.org/wiki/Unitary_matrix. [Accessed 10 07 2015].

[65] "Hermitian matrix," [Online]. Available: https://en.wikipedia.org/wiki/Hermitian_matrix. [Accessed 10 07 2015].

[66] "Orthogonal matrix," [Online]. Available: https://en.wikipedia.org/wiki/Orthogonal_matrix. [Accessed 10 07 2015].

[67] "Skew-symmetric matrix," [Online]. Available: https://en.wikipedia.org/wiki/Skew-symmetric_matrix. [Accessed 10 07 2015].

[68] B. J.S., "On the Einstein Podolsky Rosen Paradox," *Physics*, vol. 1, no. 3, pp. 195-200, 1964.

[69] "Conservation of energy," [Online]. Available: https://en.wikipedia.org/wiki/Conservation_of_energy. [Accessed 19 07 2015].

[70] "Planck time," [Online]. Available: https://en.wikipedia.org/wiki/Planck_time. [Accessed 20 07 2015].

[71] "Heisenberg picture," [Online]. Available: https://en.wikipedia.org/wiki/Heisenberg_picture. [Accessed 25 07 2015].

[72] J. Bell, Speakable and unspeakable in quantum mechanics, Cambridge: University Press, 1989.

[73] D. Chopra, "Physics May Stonewall, But Reality Doesn't," 2015. [Online]. Available: https://www.deepakchopra.com/blog/article/5438.

[74] "Temperature," 1 03 2016. [Online]. Available: https://en.wikipedia.org/wiki/Temperature.

[75] "Copenhagen Interpretation," 10 2016. [Online]. Available: https://en.wikipedia.org/wiki/Copenhagen_interpretation.

[76] "Copenhagen Interpretation," 2016. [Online]. Available: https://en.wikipedia.org/wiki/Copenhagen_interpretation.

[77] "Cool Cosmos at IPAC, NASA," 1 3 2016. [Online]. Available: http://coolcosmos.ipac.caltech.edu/cosmic_classroom/light_lessons/thermal/temperature.html.

[78] C. Wu, E. Ambler, R. Hayward, D. Hoppes and R. Hudson, "Experimental test of parity conservation in beta decay," *Phys. Rev.*, vol. 105, no. 4, pp. 1413-1415, 1957.

[79] S. Viznyuk, "Gravity-induced decay," 2016. [Online]. Available: https://www.academia.edu/21674738/Gravity-induced_decay.

[80] S. Viznyuk, "OEIS sequence A210238," 2012. [Online]. Available: http://oeis.org/A210238. [Accessed 21 04 2015].

[81] S. Viznyuk, "OEIS sequence A213008," 2012. [Online]. Available: https://oeis.org/A213008. [Accessed 21 04 2015].

[82] P. Busch, "The Time-Energy Uncertainty Relation," *arXiv:quant-ph/0105049*, 2007.

[83] P. G. Giacosa F., "Influence of the measurement on the decay law: the bang-bang," *arXiv:1411.2255v1 [quant-ph]*, 11 2014.

[84] C. Unnikrishnan, "End of Several Quantum Mysteries," *arXiv:1102.1187v1 [quant-ph],* 2 2011.

[85] T. Padmanabhan, "Thermodynamical Aspects of Gravity: New insights," *arXiv:0911.5004 [gr-qc],* 11 2009.

[86] T. Jacobson, "Thermodynamics of Spacetime: The Einstein Equation of State," *arXiv:gr-qc/9504004,* 4 1995.

[87] D. Fixen, "The Temperature of the Cosmic Microwave Background," *arXiv:0911.1955 [astro-ph.CO],* 11 2009.

[88] D. Haddad, F. Seifert, L. Chao, A. Possolo, D. Newell, J. Pratt, C. Williams and S. Schlamminger, "Measurement of the Planck constant at the National Institute of Standards and Technology from 2015 to 2017," *Metrologia,* vol. 54, no. 5, pp. 633-641, 2017.

[89] "CMB measured intensity vs frequency," NASA Goddard Space Flight Center, 2017. [Online]. Available: https://asd.gsfc.nasa.gov/archive/arcade/cmb_intensity.html. [Accessed 2017].

$N = 1000;\ M = 2;$ $\{p_i\} = \{\frac{1}{2}, \frac{1}{2}\}$		$N = 900;\ M = 3;$ $\{p_i\} = \{\frac{1}{3}, \frac{1}{3}, \frac{1}{3}\}$		$N = 600;\ M = 5;$ $\{p_i\} = \{\frac{1}{5}, \frac{1}{5}, \frac{1}{5}, \frac{1}{5}, \frac{1}{5}\}$		$N = 189;\ M = 7;$ $\{p_i\} = \{\frac{1}{7}, \frac{1}{7}, \frac{1}{7}, \frac{1}{7}, \frac{1}{7}, \frac{1}{7}, \frac{1}{7}\}$	
$\mathcal{E}$	$g(\mathcal{E}; N, \{p_i\})$	$\mathcal{E}$	$g(\mathcal{E}; N, \{p_i\})$	$\mathcal{E}$	$g(\mathcal{E}; N, \{p_i\})$	$\mathcal{E}$	$g(\mathcal{E}; N, \{p_i\})$
0.000000	1	0.000000	1	0.000000	1	0.000000	1
0.001998	2	0.003328	6	0.008299	20	0.036368	42
0.007992	2	0.009972	3	0.016598	30	0.072735	210
0.017982	2	0.009994	3	0.024828	30	0.107827	105
0.031968	2	0.013311	6	0.024966	30	0.109103	140
0.049951	2	0.023262	6	0.033127	20	0.110476	105
0.071930	2	0.023328	6	0.033196	20	0.144194	420
0.097905	2	0.029951	6	0.033265	20	0.145567	42
0.127878	2	0.039846	3	0.041495	120	0.146843	420
0.161847	2	0.040023	3	0.049521	20	0.180562	105
0.199813	2	0.043196	6	0.050072	20	0.181935	840
0.241778	2	0.043329	6	0.057889	60	0.183211	105
0.287740	2	0.053246	6	0.058024	30	0.213187	140
0.337700	2	0.063064	6	0.058162	30	0.215653	105
0.391659	2	0.063396	6	0.058302	60	0.218302	1260
0.449618	2	0.069775	6	0.066188	60	0.220951	105
0.511576	2	0.069997	6	0.066393	30	0.223804	140
0.577534	2	0.083198	6	0.066601	60	0.249555	210
0.647492	2	0.089556	3	0.074556	60	0.250928	210
0.721452	2	0.090154	3	0.074696	20	0.253394	630
[...]	[...]	[...]	[...]	[...]	[...]	[...]	[...]
640.1354	2	952.5446	6	929.0220	30	333.7789	105
644.8379	2	955.9414	3	929.4275	60	334.1844	210
649.6592	2	956.3468	6	930.8138	20	335.5707	42
654.6150	2	957.7331	6	934.0276	20	337.6184	140
659.7260	2	962.0473	6	934.7208	60	338.3115	210
665.0203	2	963.1459	6	935.8194	20	339.4101	42
670.5388	2	968.1543	3	940.4212	30	342.8495	105
676.3459	2	968.8474	6	941.1144	20	343.5426	42
682.5595	2	974.9556	6	946.8165	20	348.0859	42
689.4673	2	981.7580	3	953.2134	5	353.3277	7

Table 1

$\mathcal{E}$, $g(\mathcal{E}; N, \{p_i\})$ value pairs calculated from (9) for four sets of parameters $N, \{p_i\}$ using [18] algorithm for finding partitions $\{n_i\}$ of integer N into $\leq M$ parts. For each partition $\{n_i\}$ I calculated the value of $\mathcal{E}$ and multiplicity $D(\mathcal{E}; N, M)$ of multinomial coefficient in (4) [80]. Finally, $g(\mathcal{E}; N, \{p_i\}) = SUM(D)$ for each distinct value of $\mathcal{E}$ produced the results for the table. I display the first 20 and the last 10 records from the table.

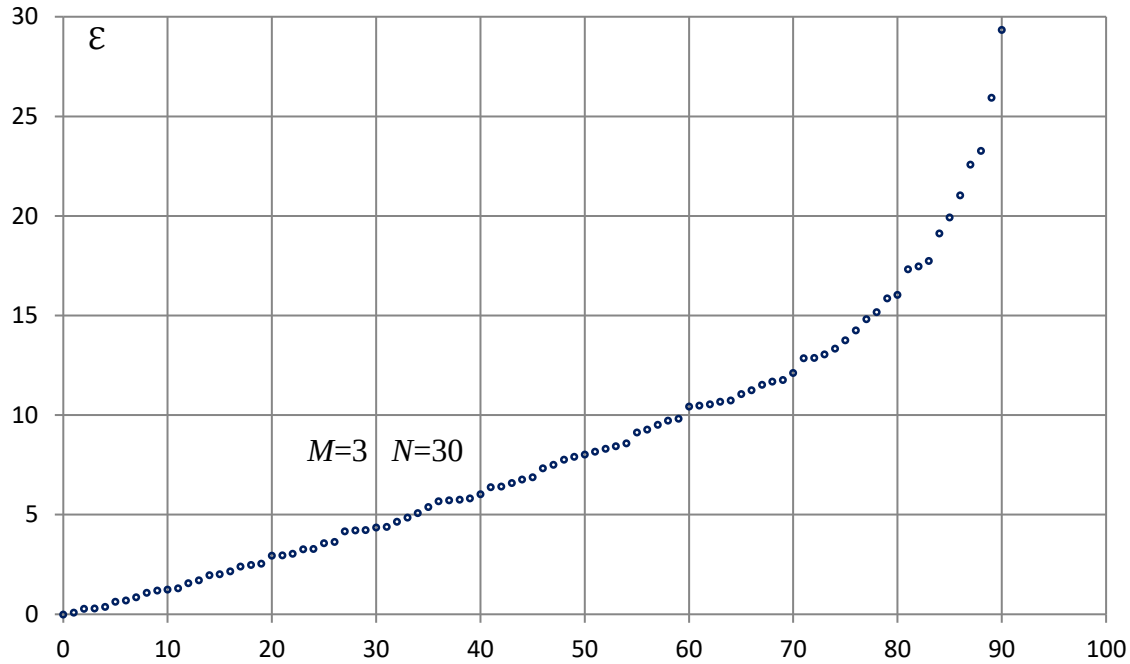

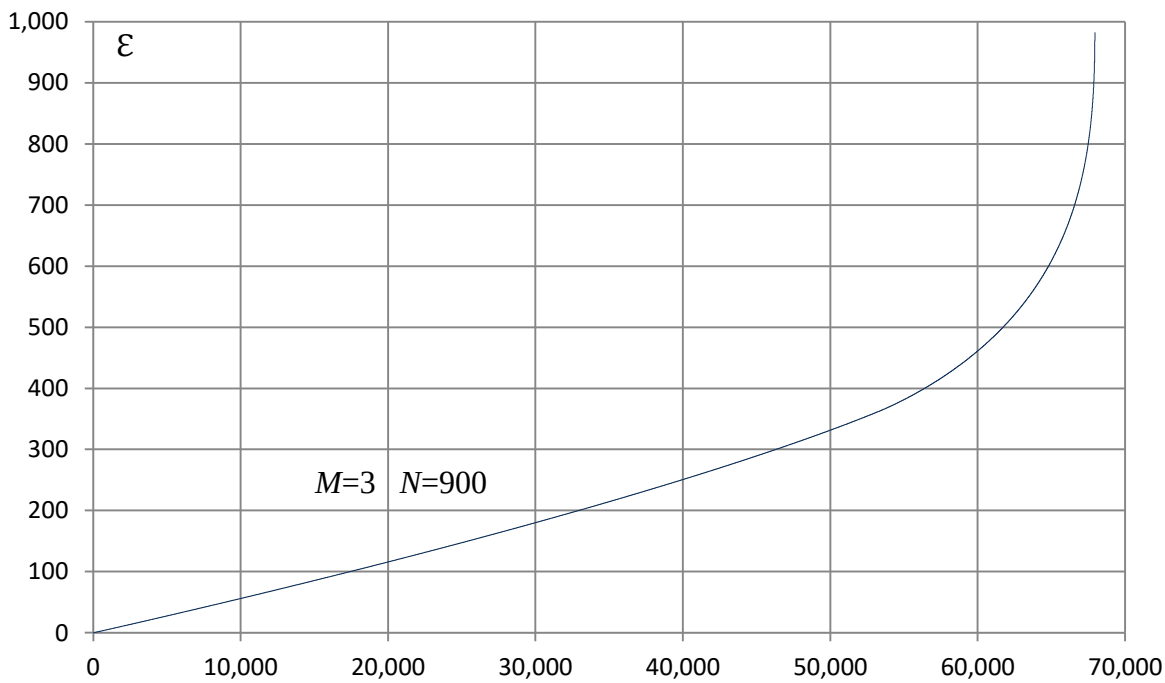

Figure 1

Distinct values of $\mathcal{E}$ in increasing order calculated from (9) with (5) and (1), using [18] algorithm for finding partitions (n_i) of integer N into $\leq M$ parts. The values of M and N are given on the graphs. The graphs represent complete set of distinct values of $\mathcal{E}$ for the given values of M and N. The graphs demonstrate close to linear dependence of $\mathcal{E}$ on "quantum number" in the vicinity of equilibrium $\mathcal{E} = 0$ for statistical ensembles with M=3. This is the characteristic feature of statistical ensemble of cardinality M=3. Away from equilibrium and close to the boundary of hyper-plane (1) the linear behavior is violated.

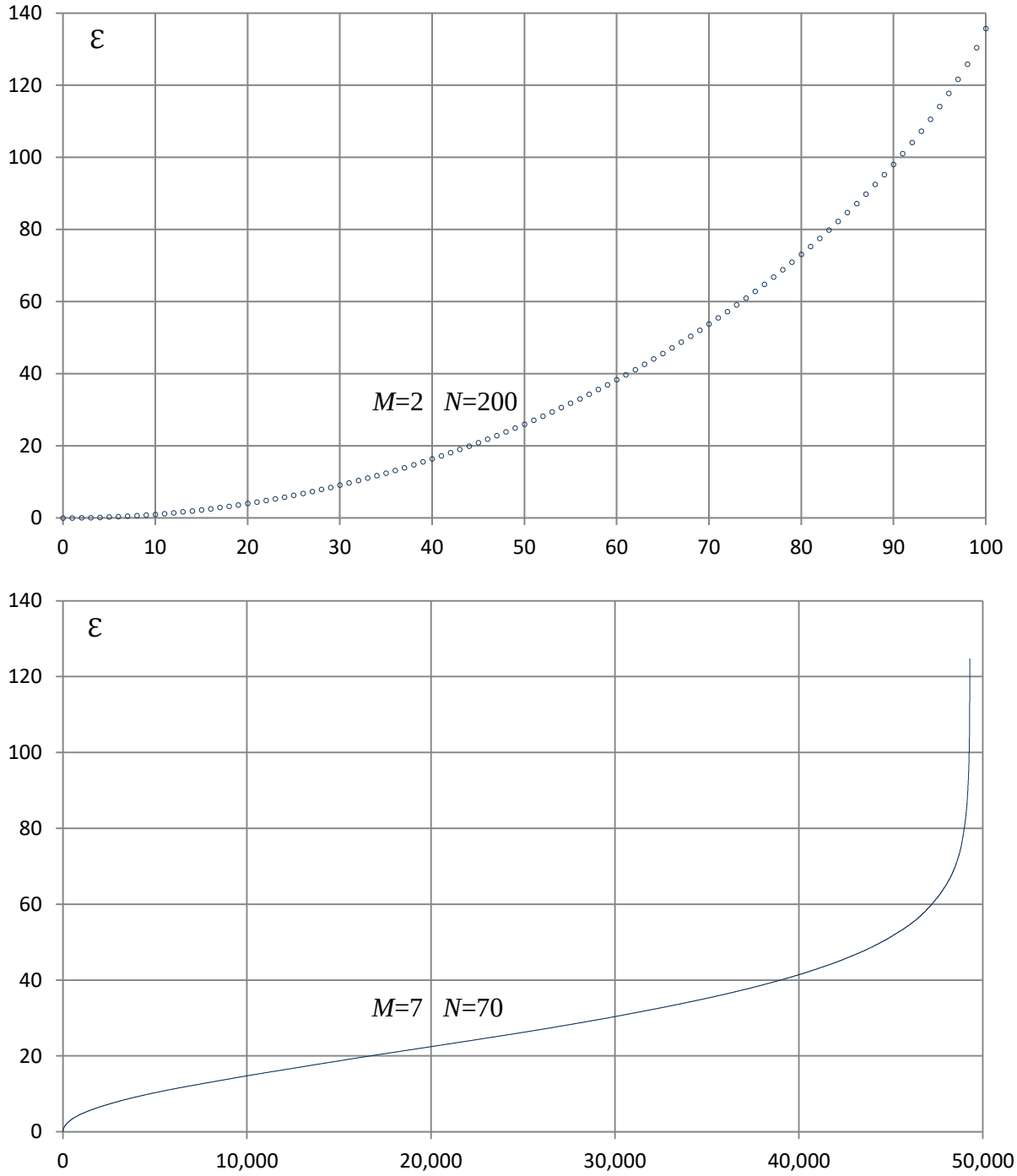

Figure 2

Distinct values of $\mathcal{E}$ in increasing order calculated from (9) with (5) and (1), using [18] algorithm for finding partitions (n_i) of integer N into $\leq M$ parts. The values of M and N are given on the graphs. The graphs represent complete set of distinct values of $\mathcal{E}$ for the given values of M and N.

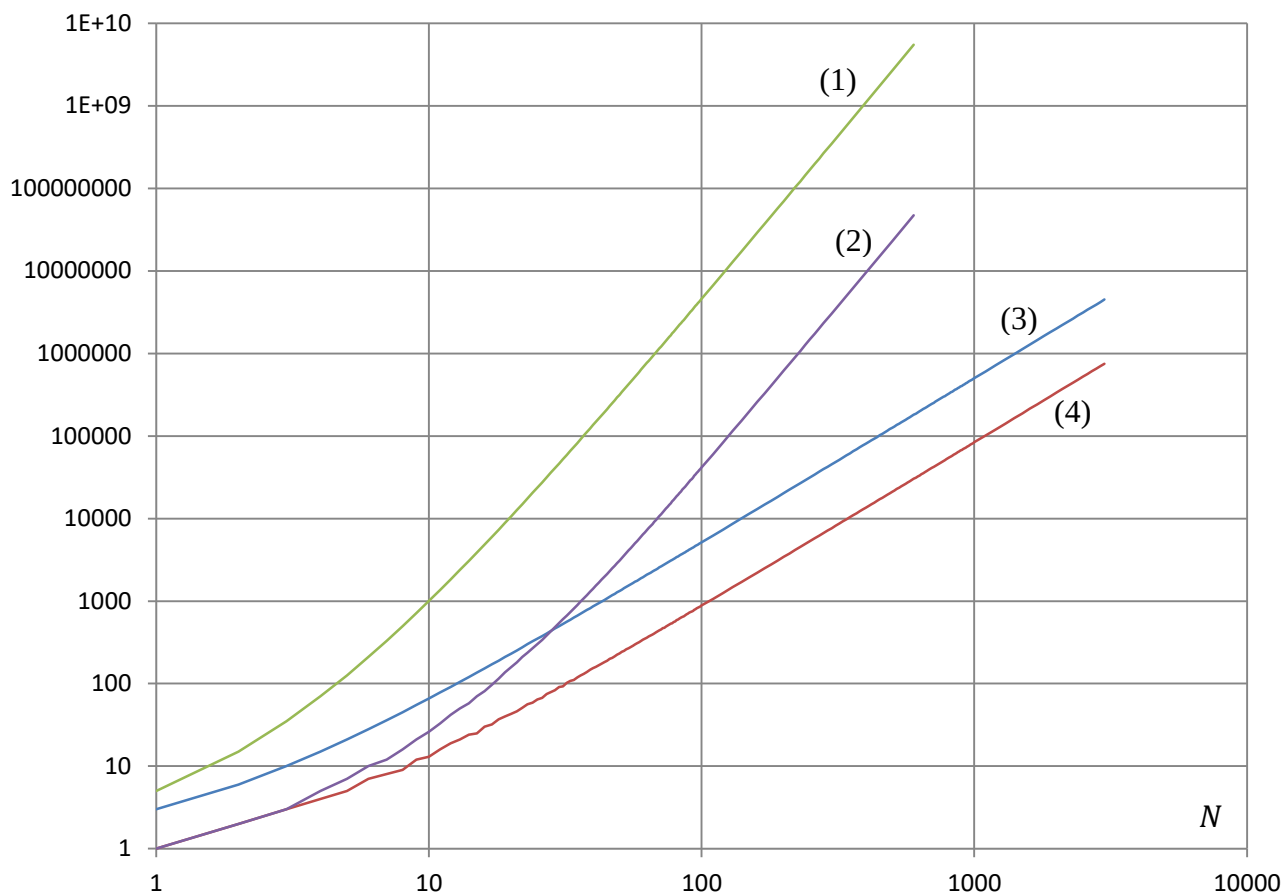

Figure 3

The total number $L(N, M)$ of distinguishable states of statistical ensemble (curves 1, 3), and the total number $\sum_{\{\mathcal{E}\}} 1$ of distinct $\{\mathcal{E}\}$ values (curves 2, 4) as functions of N for two sets of probabilities (5):

1. $L(N, M)$ for $M = 5$
2. $\sum_{\{\mathcal{E}\}} 1$ for $M = 5$
3. $L(N, M)$ for $M = 3$
4. $\sum_{\{\mathcal{E}\}} 1$ for $M = 3$

The values on curve 1 are by factor $M! = 5!$ greater than on curve 2 as $N \to \infty$. The values on curve 3 are by factor $M! = 3!$ greater than on curve 4 as $N \to \infty$.

Using Stirling's approximation for large N in formula (13) one can see the curves grow proportionally to N^{M-1} as $N \to \infty$

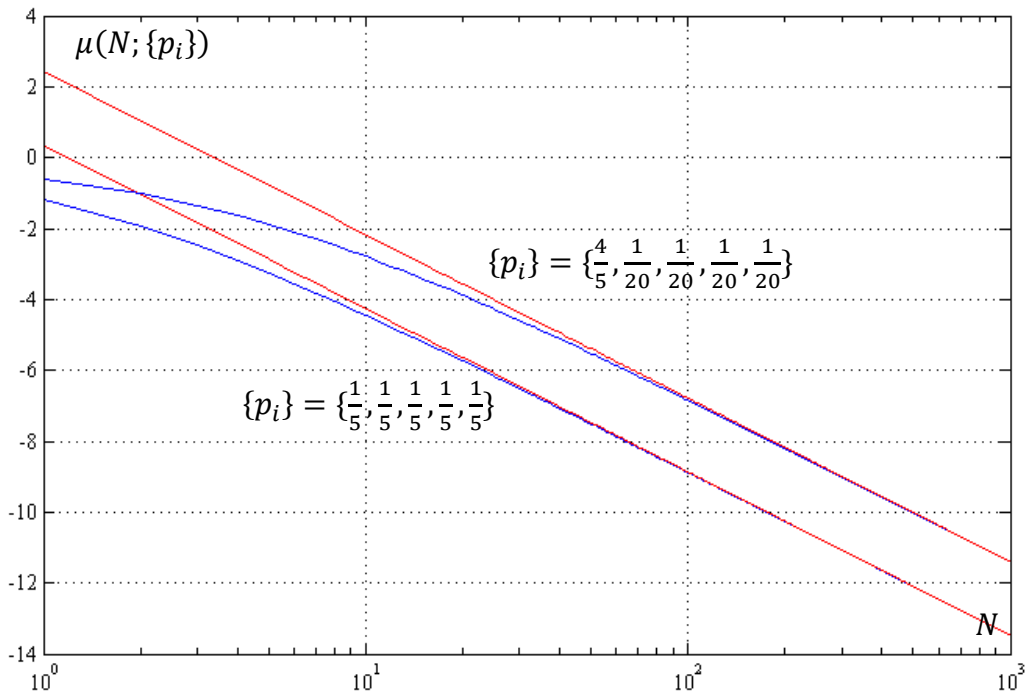

Figure 4
Function $\mu(N;\{p_i\})$ calculated for two sets of probabilities $\{p_i\}$. Blue lines were calculated using exact formula (7). Red lines were calculated using thermodynamic limit approximation (17)

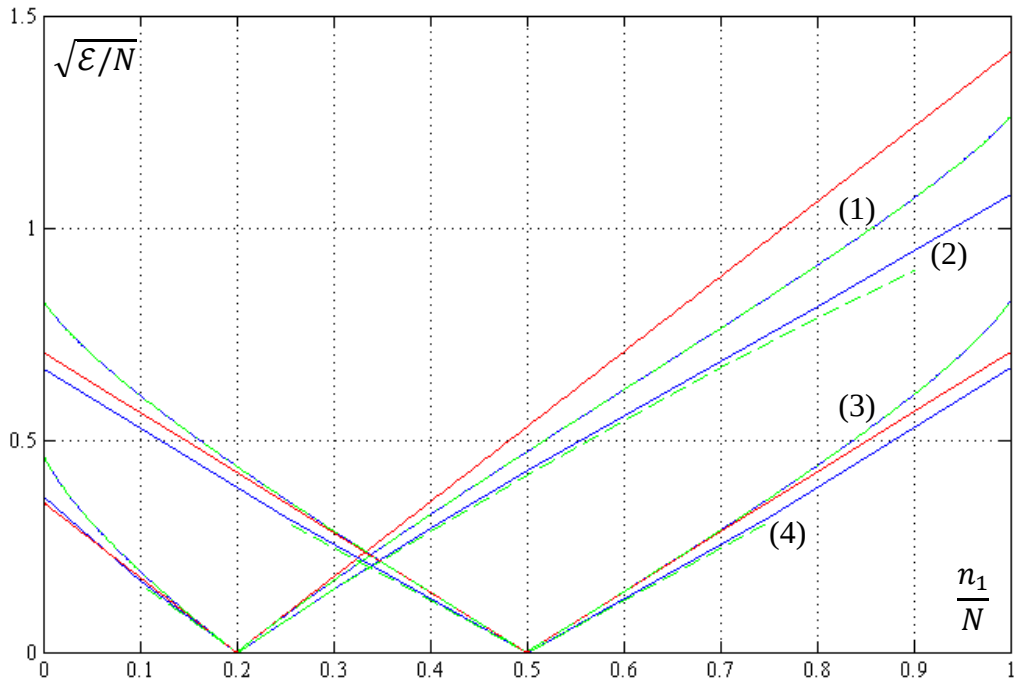

Figure 5

Values of $\sqrt{\mathcal{E}/N}$ calculated as a function of n_1/N with probabilities (5) for four sets of parameters:

1. $M = 5;\ N = 1000$
2. $M = 5;\ N = 10$
3. $M = 2;\ N = 1000$
4. $M = 2;\ N = 4$

Blue lines were calculated using exact formula (9). Green dash lines were calculated using thermodynamic limit approximation (18). Red lines were calculated using quadratic form (24) approximation. For a given value of n_1 the values $\{n_{i>1}\}$ were distributed proportionally to corresponding probabilities $\{p_{i>1}\}$. For large value of $N = 1000$ the blue lines and green dash lines overlap closely as seen on curves 1 and 3. For small values of N the thermodynamic limit approximation is not accurate, and blue lines differ from green dash lines as seen on curves 2 and 4. Red lines overlap with blue lines in close proximity to the minimum (10) of $\mathcal{E}$.

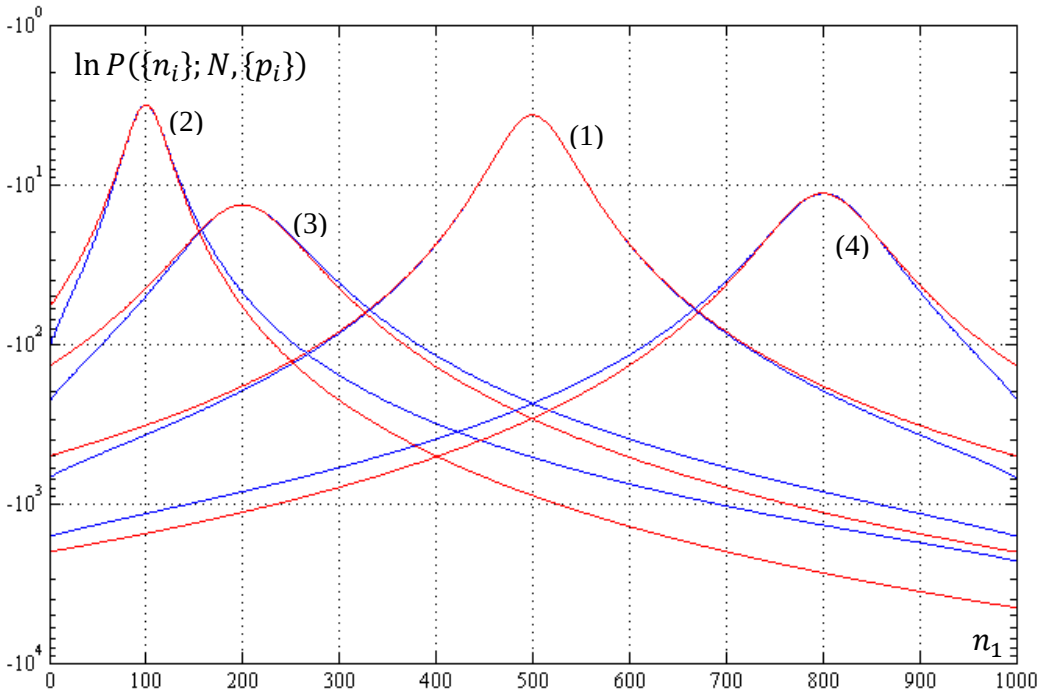

Figure 6

Values of $\ln P(\{n_i\}; N, \{p_i\})$ calculated as a function of n_1 for $N = 1000$ and four sets of probabilities $\{p_i\}$

1. $\{p_i\} = \left\{\frac{1}{2}, \frac{1}{2}\right\}$
2. $\{p_i\} = \left\{\frac{1}{10}, \frac{9}{10}\right\}$
3. $\{p_i\} = \left\{\frac{1}{5}, \frac{1}{5}, \frac{1}{5}, \frac{1}{5}, \frac{1}{5}\right\}$
4. $\{p_i\} = \{\frac{4}{5}, \frac{1}{20}, \frac{1}{20}, \frac{1}{20}, \frac{1}{20}\}$

Blue lines were calculated using exact formula (4). Red lines were calculated using multivariate normal approximation (28). For the given value of n_1 the distribution of values $\{n_{i>1}\}$ is proportional to the corresponding probabilities $\{p_{i>1}\}$

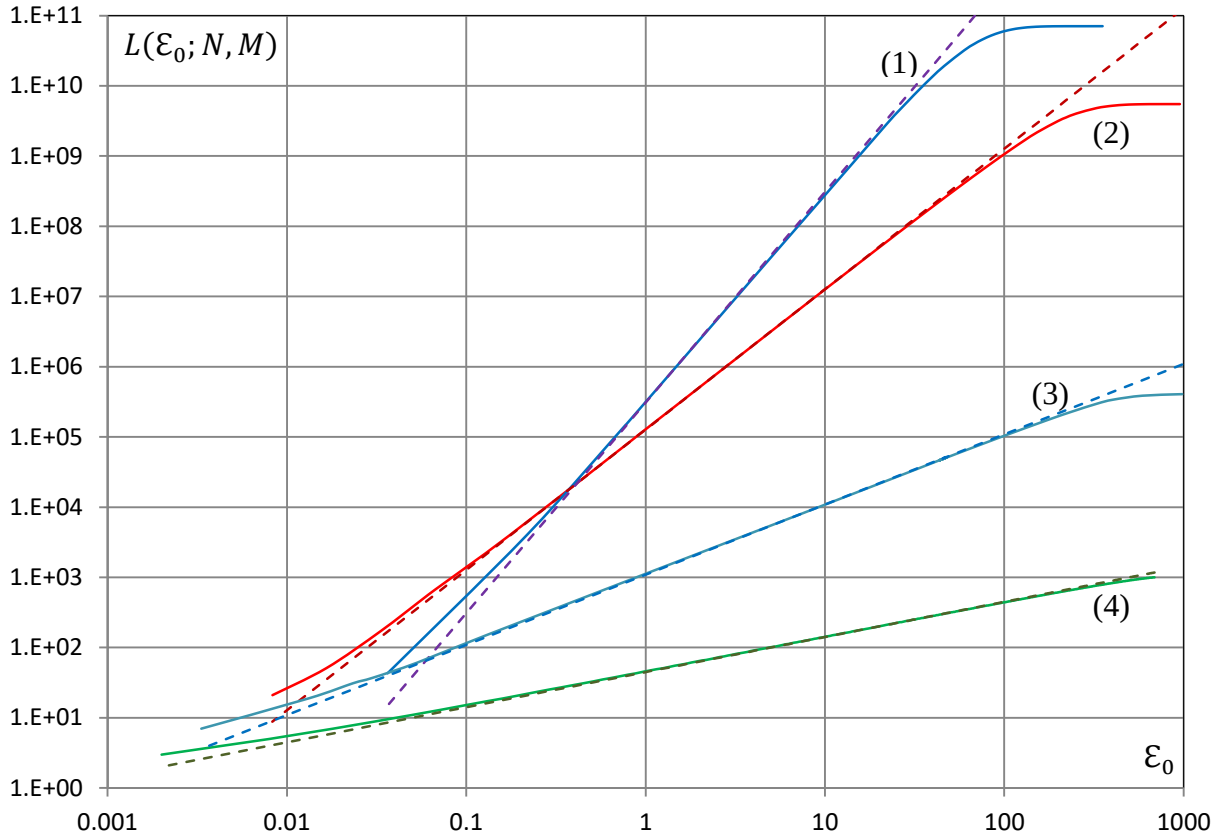

Figure 7

The number of distinguishable states $L(\mathcal{E}_0; N, M)$ of statistical ensemble having $\mathcal{E} \leq \mathcal{E}_0$ as a function of $\mathcal{E}_0$ for three sets of the parameters and probabilities (5):

1. $M = 7;\ N = 189$
2. $M = 5;\ N = 600$
3. $M = 3;\ N = 900$
4. $M = 2;\ N = 1000$

Solid lines are the results of calculation using exact formulas (4) and (9). Dash lines represent thermodynamic limit approximation (36). The graphs demonstrate thermodynamic limit provides the better approximation the larger is the ratio N/M. Solid lines level off close to $\mathcal{E}_{max}$ because density of states per interval $d\mathcal{E}$ decreases near $\mathcal{E}_{max}$ due to non-spherical $\mathcal{E}$-domain boundary of hyper-plane (1). The boundary is defined by $n_i \geq 0\ \forall\ \boldsymbol{i} \in \boldsymbol{G}$

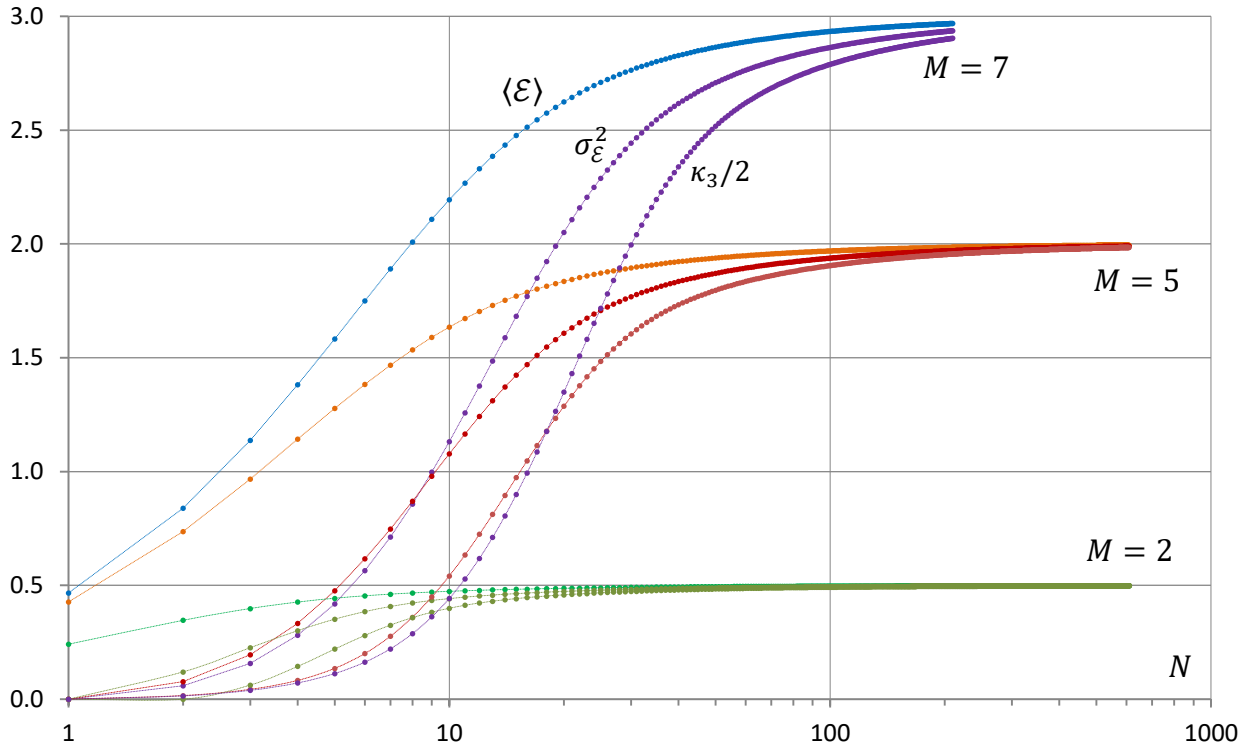

Figure 8

The mean value $\langle\mathcal{E}\rangle$, the variance $\sigma_{\mathcal{E}}^2$, and the third moment κ_3 vs. total number N of microstates for three values of M and probabilities (5). The graphs have been calculated using exact expressions (42-44) with probability mass function (4). The value of the third moment κ_3 is reduced by a factor of 2 to show its asymptotic behavior comparing with $\langle\mathcal{E}\rangle$ and $\sigma_{\mathcal{E}}^2$. For each set of parameters, the curves approach $(M-1)/2$ values as $N \cdot p_i \to \infty$

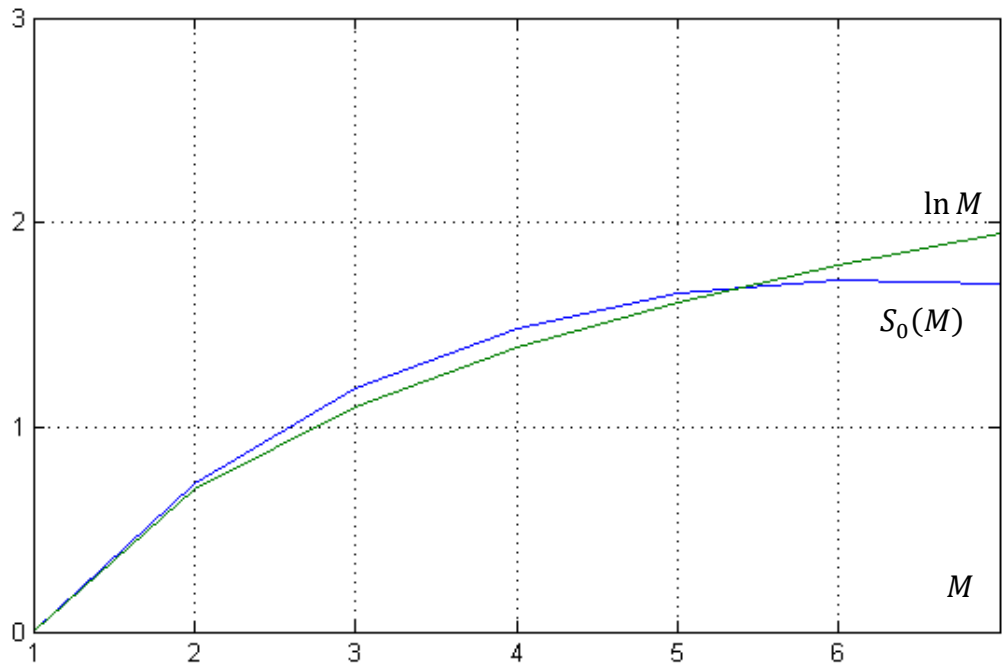

Figure 9
Comparison of $S_0(M)$ in (76) with $\ln M$

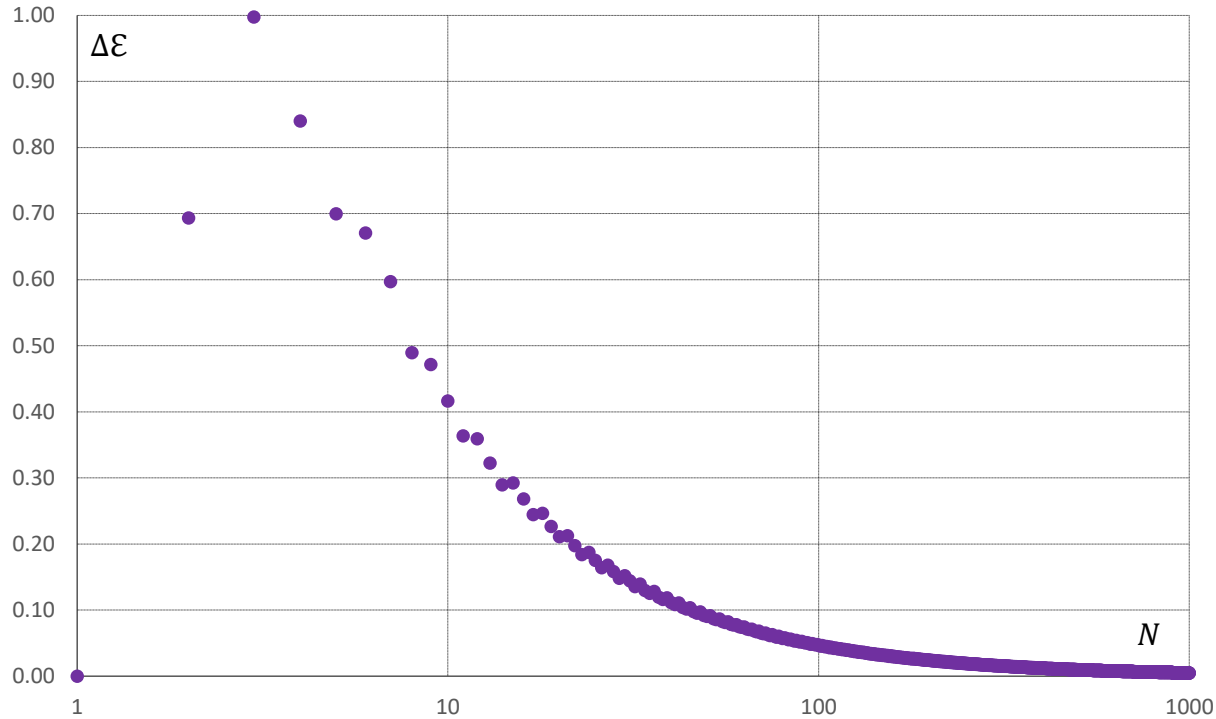

Figure 10

Difference $\Delta\mathcal{E}$ between adjacent energy levels (9), averaged over distinct states of statistical ensemble with the given value of N, and $M = 3$. The curve is approximated by (78) as $N \to \infty$

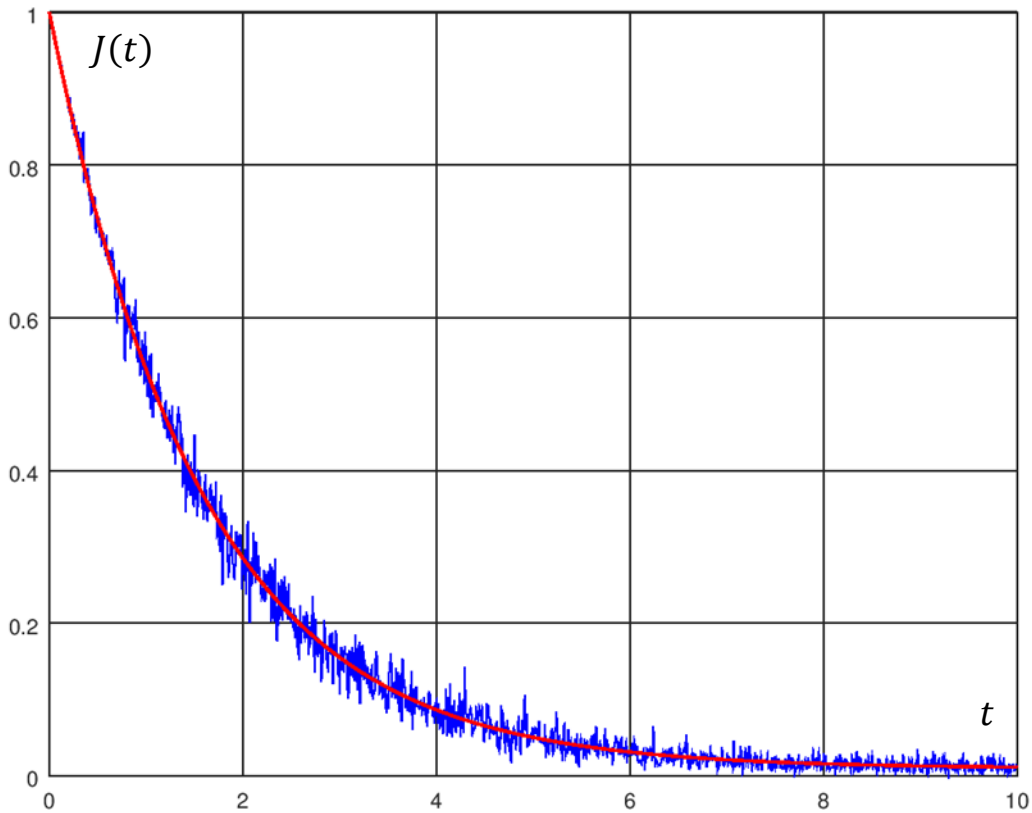

Figure 11

Blue line is a calculation of measurement scalar (106), with binomially distributed phases $\varphi_{\{\boldsymbol{y}_i\}}$, as a function of time t. The red line is a plot of formula (114). The plots have been produced using GNU Octave (MATLAB) code http://phystech.com/download/ph.m with the following parameters:

- number of knowledge vectors in superposition $\boldsymbol{y} = \sum \boldsymbol{y}_i;\ K = 100$
- mean free time between transitions of a knowledge vector $\boldsymbol{y}_i$: $\tau = 0.01$
- characteristic frequency $\omega = 8$

The plots have been normalized to 1. As the number of knowledge vectors K increases the blue curve smoothers and becomes identical with red curve.